RSC Advances

PAPER

View Article Online
View Journal | View Issue

Cite this: *RSC Adv.*, 2025, **15**, 14859

Computational and experimental approach for investigating the microstructural parameters of a cadmium indium selenide (α-$CdIn_2Se_4$) ternary semiconducting compound

S. D. Dhruv,[a] Sergei A. Sharko,[b] Aleksandra I. Serokurova,[b] Nikolai N. Novitskii,[b] D. L. Goroshko,[c] Parth Rayani,[d] Jagruti Jangale,[a] Naveen Agrawal,[a] Vanaraj Solanki,[f] J. H. Markna,[e] Bharat Kataria[e] and D. K. Dhruv *[a]

Several properties are carefully considered before choosing a semiconducting material for the fabrication of a thin-film electronic device. Cadmium indium selenide ($CdIn_2Se_4$) is a ternary semiconducting compound belonging to the II–III_2–VI_4 family, where II = zinc (Zn), cadmium (Cd), or mercury (Hg); III = aluminium (Al), gallium (Ga), or indium (In); and VI = sulphur (S), selenium (Se), or tellurium (Te). The Cambridge serial total energy package (CASTEP) module, within the framework of density functional theory (DFT) using the PBE-GGA (Perdew–Burke–Ernzerhof generalized gradient approximation), was used to compute the elastic constants for the $CdIn_2Se_4$ ternary semiconducting compound. Stoichiometric amounts of 5 N-pure (99.999%) Cd, In, and Se elements were used to synthesize the $CdIn_2Se_4$ compound using a microcontroller-based programmable high-temperature rotary furnace. X-ray diffraction (XRD) was used to examine the crystal structure and phase purity of the synthesized $CdIn_2Se_4$ ternary semiconducting compound. The synthesized $CdIn_2Se_4$ ternary semiconducting compound exhibited a high level of crystallinity, as evinced by its strong XRD peak intensity and narrow full width at half maximum (FWHM, β) of the diffraction peaks. Identification, indexing, and accurate mapping of the X-ray diffractogram peaks of $CdIn_2Se_4$ were successfully performed using ICDD card No. 01-089-2388. The synthesized $CdIn_2Se_4$ ternary semiconducting compound possessed a single-phase pseudo-cubic α-phase tetragonal structure ($c \simeq a$) with the $P\bar{4}2m$(111) crystallographic space group (SG). For the most prominent XRD peak (111), the stacking fault (SF) value of the ternary semiconducting compound $CdIn_2Se_4$ was determined to be 1.0267 $\times$ 10^{-3}. For the preferred orientations of the crystallites along a crystal plane (*hkl*), the texture coefficient (C_i) of each XRD peak of the ternary semiconducting compound $CdIn_2Se_4$ was measured, yielding values close to unity ($\simeq$1). The degree of preferred orientation (Δ) for the ternary semiconducting compound $CdIn_2Se_4$ was found to be 9.6751 $\times$ 10^{-4}. To gain insight into the growth behavior of the synthesized $CdIn_2Se_4$ ternary semiconducting compound, the Bravais theory was applied to compute the *d*-interplanar spacings (d_{hkl}), enabling inference on the significance of the (111) plane in the crystal structure of $CdIn_2Se_4$. The lattice constant (*a*) for the $CdIn_2Se_4$ ternary semiconducting compound was 0.5818 nm, corresponding to a cell volume of 0.1969 nm^3, calculated using the Miller indices for the prominent (111) plane. Rietveld refinement (RR) of the XRD data for the ternary semiconducting compound $CdIn_2Se_4$ was performed using the FullProf Suite software. Several microstructural parameters of the $CdIn_2Se_4$ compound, including lattice parameter (*a*), crystallite size (*D*), lattice strain (ε), root mean square strain (ε_{rms}), dislocation density (δ), lattice stress (σ), and energy density (*u*), were determined. Additionally, bulk modulus (B_H), shear modulus (G_H), Young's modulus (*y*), Poisson's ratio (ν), elastic anisotropy, melting temperature (T_m), transverse sound velocity (v_t), longitudinal sound velocity (v_l), average wave velocity (v_m),

Received 15th March 2025
Accepted 17th April 2025

DOI: 10.1039/d5ra01850a

rsc.li/rsc-advances

[a]*Natubhai V. Patel College of Pure and Applied Sciences, The Charutar Vidya Mandal (CVM) University, Vallabh Vidyanagar 388120, Gujarat, India. E-mail: dhananjaydhruv@rediffmail.com*

[b]*Laboratory of Magnetic Films Physics, Scientific-Practical Materials Research Centre of National Academy of Sciences of Belarus, 220072 Minsk, Belarus*

[c]*Institute of Automation and Control Processes Far Eastern Branch of the Russian Academy of Sciences, 5 Radio St., Vladivostok 690041, Russia*

[d]*Government Science College, Maharaja Krishnakumarsinhji Bhavnagar University, Gariyadhar, Bhavnagar 364505, Gujarat, India*

[e]*Department of Nanoscience and Advanced Materials, Saurashtra University, Rajkot 360005, Gujarat, India*

[f]*Dr. K. C. Patel R & D Centre, Charotar University of Science and Technology, Changa 388421, Gujarat, India*

and Debye temperature (θ_D) were derived for the $CdIn_2Se_4$ compound. Energy dispersive X-ray analysis (EDAX) with elemental mapping and a densitometer (pycnometer) confirmed the stoichiometry (with elemental distribution) and density (ρ) of the synthesized $CdIn_2Se_4$ compound, respectively. Room temperature (RT) ($\simeq$300 K) Fourier transform infrared (FTIR) spectroscopy in the wavenumber ($\bar{\nu}$) range of 4000–400 cm^{-1} confirmed the purity of the synthesized $CdIn_2Se_4$ ternary semiconducting compound by detecting the presence of functional group/s, if any, in the FTIR spectra. The findings obtained from the detailed investigation of the $CdIn_2Se_4$ compound may serve as a valuable reference for future researchers focused on device development. Accordingly, the authors have made a concerted effort to examine various properties of the $CdIn_2Se_4$ ternary semiconducting compound through both theoretical and experimental approaches. It is anticipated that researchers worldwide may utilize these results in the development of a wide range of electronic devices. The implications of the study are discussed.

1. Introduction

A review of the literature on the synthesis of II–III_2–VI_4 ternary semiconducting compounds (where II = zinc (Zn), cadmium (Cd), or mercury (Hg); III = aluminium (Al), gallium (Ga), or indium (In); VI = sulphur (S), selenium (Se), or tellurium (Te)) reveals that many researchers have investigated the growth of II–III_2–VI_4 compounds using numerous techniques. These include the fusion of II, III, and VI group elements (FC) or binary II–VI and III_2–VI_3 compounds (FBC), chemical transport reactions (CTRs), growth from the melt (GM), zone melting (ZM), and others.[1–5] These materials are considered promising for optoelectronic devices,[6–8] memory switching devices,[9,10] and more.

A polycrystalline ingot of cadmium indium selenide ($CdIn_2Se_4$) was prepared by the direct fusion of stoichiometric amounts of their constituting elements cadmium (Cd), indium (In), and selenium (Se) by Tomkiewicz *et al.*[11] The binary component of CdSe and In_2Se_3 in stoichiometric proportions was used by El-Zaidia *et al.*[2] and El-Nahass *et al.*[12] to prepare a $CdIn_2Se_4$ bulk by the direct fusion method. Stoichiometric single crystals of tetragonal (pseudo-cubic) $CdIn_2Se_4$ were grown by the chemical vapour transport (CVT) method using iodine as a transport agent by Santamaría-Pérez *et al.*,[3] Neumann *et al.*,[13,14] Razzetti *et al.*,[15] Fornarini *et al.*,[16] Trykozko *et al.*,[17] Margaritondo *et al.*,[18] and Przedmojski *et al.*[19] Adpakpang *et al.*[20] have synthesized a $CdIn_2Se_4$ powder *via* aqueous chemical reduction (solution method). Ruanthon *et al.*[21] have prepared a $CdIn_2Se_4$ compound by a sol–gel method. Choe *et al.*[22] and Kerimova *et al.*[23] have grown $CdIn_2Se_4$ single crystals by the vertical Bridgman technique. Guerrero *et al.*[24] have grown the $CdIn_2Se_4$ compound by a melt-and-anneal technique. Fortin *et al.*[25] and Nitsche *et al.*[26] have grown $CdIn_2Se_4$ compounds by chemical transport.

Bulk modulus, elastic constants, and force constants of interatomic bonds of II–III_2–VI_4 compounds were scrutinized by Mamedova *et al.*[27] and Chandra *et al.*[28] by using *ab initio* density functional perturbation theory. Priyambada *et al.*[29] and Hoat *et al.*[30] have explored the exhaustive structural, electronic, elastic, mechanical, and thermoelectric chattels of defect $CdIn_2Se_4$ chalcopyrite-type semiconductor using an *ab initio* slant within the density functional theory (DFT) along with the semi-classical Boltzmann transport theory. The results obtained by Hoat *et al.*[30] reveal that $CdIn_2Se_4$ is a promising absorber to work under ultraviolet radiation, and thermoelectric parameters such as Seebeck coefficient, electrical conductivity, electronic thermal conductivity, power factor, and dimensionless figure of merit were estimated. Only Santamaria-Perez *et al.*[3] have steered both experimental and theoretical studies on $CdIn_2Se_4$ and presented the structural and vibrational properties of $CdIn_2Se_4$ under high pressure at ambient temperature.

Ternary semiconducting compound $CdIn_2Se_4$ has engrossed much contemplation from researchers due to its claims in heterojunction solar cells,[31] photoanodes,[32] photoelectrochemical solar cells,[11,16,33–35] thermoelectric materials,[20,21] photovoltaics,[36] *etc.*

No crystal can be regarded as perfect due to its intrinsic restrictions; a perfect crystal would seem to extend indefinitely in all directions. Diffraction peak broadening is instigated by changes in materials that preserve crystallinity. The primary measurements obtained from the peak width analysis of X-ray diffraction (XRD) are crystallite size (D) and lattice strain (ε).

The extant research paper throws light on the synthesis of $CdIn_2Se_4$ ternary semiconducting compounds by melting 5 N (99.999%) pure cadmium (Cd), indium (In), and selenium (Se) constituent elements in stoichiometric proportions. The investigation determines crystallographic characteristics such as stacking faults (SF), texture coefficient (C_i), degree of preferred orientation (Δ), lattice parameters (a, b, and c), and unit cell volume (V) for the $CdIn_2Se_4$ ternary semiconducting compound. Various microstructural parameters such as crystallite size (D), lattice strain (ε), root mean square strain (ε_{rms}), dislocation density (δ), lattice stress (σ), and energy density (u) of this compound have been derived by employing the Nelson–Riley (N–R), Scherrer, Stokes–Wilson (S–W), Monshi, Williamson–Smallman (W–S), Williamson–Hall (W–H), size–strain plot (SSP), and Halder–Wagner (H–W) methods. Bulk modulus (B_H), shear modulus (G_H), Young's modulus (y), Poisson's ratio (ν), elastic anisotropy, melting temperature (T_m), transverse sound velocity (v_t), longitudinal sound velocity (v_l), average wave velocity (v_m), and Debye temperature (θ_D) have also been derived for this compound. Energy dispersive X-ray analysis (EDAX) and a densitometer (pycnometer) have verified the stoichiometry and density (ρ) of the synthesized $CdIn_2Se_4$ ternary semiconducting compound, respectively, while Fourier transform infrared (FTIR) spectroscopy has confirmed the compound's purity.

Several of the material's qualities are well-thought-out before picking a semiconducting material to construct a thin-film semiconductor electronic gizmo. Thus, the data salvaged from the $CdIn_2Se_4$ ternary semiconducting compound's detailed

studies may obligate future device development investigators. The authors, hence, tried to meticulously scrutinize the different properties of the $CdIn_2Se_4$ ternary semiconducting compound theoretically and experimentally; it is expected that researchers worldwide will use the findings for the fabrication of various devices.

2. Experimental

2.1. Computational details

The elastic constant calculations for the $CdIn_2Se_4$ ternary semiconducting compound were performed using the Cambridge serial total energy package (CASTEP, a package for performing *ab initio* quantum-mechanical atomistic simulations) module in the density functional theory (DFT) framework under the Perdew–Burke–Ernzerhof-generalized gradient approximation (PBE-GGA) approach.[37] The CASTEP calculation was performed with single-point energy calculation using the Perdew–Burke–Ernzerhof (PBE) exchange–correlation functional without spin polarization. The cut-off energy for the plane-wave basis set was set to 394.6000 eV, ensuring sufficient accuracy in the electronic structure calculations. The *k*-points were explicitly defined using the KPOINTS_LIST rather than an automatically generated grid. A total of 15 *k*-points were sampled in the Brillouin zone, with representative points such as (0.3333, 0.3333, 0.3333) and (0.3333, 0.3333, 0.0000), each assigned a weight of 0.0741. The self-consistent field (SCF) energy convergence tolerance was set to 1.0000×10^{-6} eV, with a maximum of 100 self-consistent field (SCF) cycles allowed. The Pulay mixing scheme was used for charge density mixing, with a mixing amplitude of 0.5, a mixing G_{max} of 1.5, and a mixing history length of 20 iterations. For metallic systems, the density mixing (DM) method was employed. If geometry optimizations were included, the limited-memory Broyden–Fletcher–Goldfarb–Shanno (L-BFGS or LM-BFGS) method would be used with convergence criteria of 1.0000×10^{-5} eV for energy, 0.0300 eV $Å^{-1}$ for force, 0.0500 GPa for stress, and 1.0000×10^{-3} Å for displacement, with a maximum of 100 iterations.

The elastic constant's calculations employed the stress–strain method, a widely accepted approach for determining elastic properties; this method systematically applied a series of small deformations (strains) to the crystal lattice, and the resulting stress responses were recorded. The CAmbridge Serial Total Energy Package (CASTEP) simulation involved the application of different strain patterns, each corresponding to specific components of the elastic stiffness tensor (C_{ij}). The corresponding stress tensor was computed using the Hellmann–Feynman theorem for each applied strain, ensuring an accurate representation of the $CdIn_2Se_4$ ternary semiconducting compound's elastic behaviour. The calculated stress components were then used to extract the elastic constants using a least-squares fitting method, which minimizes errors in the obtained values. The calculations were performed under high-precision settings to ensure numerical accuracy and convergence, including an appropriately chosen plane-wave cut-off energy and *k*-point sampling based on the Monkhorst–Pack scheme. The transformed stress tensors were recorded for multiple strain amplitudes, allowing for a robust evaluation of the elastic coefficients of the α-$CdIn_2Se_4$ ternary semiconducting compound. The elastic coefficients' computed values were further analyzed to obtain secondary mechanical properties such as Bulk modulus (B_H), shear modulus (G_H), Young's modulus (y), Poisson's ratio (ν), elastic anisotropy, melting temperature (T_m), transverse sound velocity (ν_t), longitudinal sound velocity (ν_l), average wave velocity (ν_m), and Debye temperature (θ_D), which provides insights into the mechanical stability of the α-$CdIn_2Se_4$ ternary semiconducting compound material and its potential applicability in developing various applications in science and technology. The formation energy of the α-(phase) $CdIn_2Se_4$ ternary semiconducting compound is −4.1118 eV per formula unit; the negative sign indicates that the synthesized α-(phase) $CdIn_2Se_4$ ternary semiconducting compound is stable and thermodynamically favourable.

The authors used the bond lengths, bond angles, and atom parameters of the ternary semiconducting compound $CdIn_2Se_4$, which were obtained using Rietveld refinement to calculate the elastic constants. The elastic stiffness constants (C_{ij}) for the ternary semiconducting compound $CdIn_2Se_4$ deduced using the CAmbridge Serial Total Energy Package (CASTEP) simulation tool are listed in Table 1.

The values of various elastic stiffness constants (C_{ij}) of ternary semiconducting compound $CdIn_2Se_4$ derive elastic compliance constants (S_{ij})

$$S_{11}\left(= \frac{C_{33}}{2C} + \frac{1}{2(C_{11} - C_{12})} = 3.7084 \times 10^{-11}\ m^2/N \right),$$

$$S_{12}\left(= \frac{C_{33}}{2C} - \frac{1}{2(C_{11} - C_{12})} = -1.7536 \times 10^{-11}\ m^2/N \right),$$

$$S_{13}\left(= -\frac{C_{13}}{C} = -1.4798 \times 10^{-11}\ m^2/N \right),$$

$$S_{33}\left(= \frac{C_{11} + C_{12}}{C} = 4.5356 \times 10^{-11}\ m^2/N \right),$$

$$S_{44}\left(= \frac{1}{C_{44}} = 4.8523 \times 10^{-11}\ m^2/N \right),$$

$$S_{55}\left(= \frac{1}{C_{55}} = 4.8523 \times 10^{-11}\ m^2/N \right), \quad \text{and}$$

$$S_{66}\left(= \frac{1}{C_{66}} = 3.8358 \times 10^{-11}\ m^2/N \right).$$

To confirm the mechanical stability of the tetragonal crystal system, the values of elastic stiffness constants (C_{ij}) should satisfy the conditions C_{11} (=59.7039 GPa) > 0, C_{33} (=43.5708 GPa) > 0, C_{44} (=20.6089 GPa) > 0, C_{66} (=26.0705 GPa) > 0, C_{11} (=59.7039 GPa) > C_{12} (=41.3956 GPa), $C_{11} + C_{33} - 2C_{13}$ (=37.3054 GPa) > 0, and $2C_{11} + C_{33} + 2C_{12} + 4C_{13}$ (=377.7082 GPa) > 0,

Table 1 Elastic stiffness constants (C_{ij}) for the ternary semiconducting compound α-$CdIn_2Se_4$ deduced using the CASTEP simulation tool

Elastic stiffness constants (C_{ij}) (GPa)	α-$CdIn_2Se_4$	β-$CdIn_2Se_4$ (ref. 29)
C_{11}	59.7039	28.7910
C_{12}	41.3956	10.8900
C_{13}	32.9847	12.1850
C_{33}	43.5708	29.3700
C_{44}	20.6089	20.2880
C_{55}	20.6089	—
C_{66}	26.0705	20.2770

suggested by the Born–Huang lattice dynamical theory,[38] which is satisfied well by the ternary semiconducting compound $CdIn_2Se_4$ (the values are written in brackets), confirming the mechanical stability of the tetragonal ternary semiconducting compound $CdIn_2Se_4$ system.

2.2. Materials and methods

2.2.1. Synthesis. Stoichiometric amounts of the elements of 5 N purity (99.999%) cadmium (Cd), indium (In), and selenium (Se) (make: Sigma-Aldrich Chemie GmbH, Germany) were used to concoct the ingot of cadmium indium selenide ($CdIn_2Se_4$). The cadmium (Cd), indium (In), and selenium (Se) concoction was sealed in a stoichiometric proportion under $\simeq 10^{-4}$ Pa pressure (vacuum) in a painstakingly cleaned quartz glass ampoule (length: $\simeq$0.15 m and diameter: $\simeq$0.015 m). The evacuated and sealed quartz glass ampoule was placed inside the microcontroller-based programmable high-temperature rotary furnace (model: RTF1000, Make: Naskar, India) and allowed to stay in the constant temperature zone. The ampoule was heated gradually ($\simeq$325 K h^{-1}) (ramp rate) to prevent explosions at high temperatures caused by the different vapour pressures of cadmium (Cd), indium (In), and selenium (Se) elements, according to the Clausius–Clapeyron equation.[39] The charge (mixture of all three elements) was heated to a temperature of $\simeq$1275 K above the melting point of $CdIn_2Se_4$ (the melting point of $CdIn_2Se_4$ is $\simeq$1193.15 K[40]). An ample homogenization could be accomplished by keeping the melt at $\simeq$1275 K for $\simeq$15 hours (dwell time). During the dwell time, the ceramic muffle was rotated ($\simeq$10 rpm) using a stepper motor for improved mixing of the cadmium (Cd), indium (In), and selenium (Se) elements. To dodge cracking/breaking due to the thermal expansion of the melt during the solidification, the quartz glass ampoule was cooled leisurely ($\simeq$285 K h^{-1}) (ramp rate) to room temperature (RT) ($\simeq$300 K), and the lower cooling rate also benefits in conquering better crystallization. A quartz glass ampoule was placed in the furnace with a small height gradient to achieve charge nucleation at the ampoule's end. Subsequently, a greyish ingot is bent when the ampoule is wrecked. The ensuing ingot was transformed into a fine powder by crushing it in a small agate mortar to have a smooth, continuous diffraction pattern in the X-ray diffraction (XRD) study.

2.2.2. Characterization. Using emblematic Cu Kα radiation ($\lambda \simeq 0.1541$ nm) in the diffraction angle (2θ) range of 20° to 80°, X-ray diffraction (XRD) (model: X'Pert MPD; Make: Philips, Holland) was used to foresee the crystal structure of the semiconducting bulk material $CdIn_2Se_4$. The synthesized compound's stoichiometry and elemental mapping were ingrained by energy-dispersive analysis of X-ray (EDAX) scrutiny (model: Xflash7, make: Bruker, Germany). A densitometer (pycnometer) (model: SMART PYCNO 30, Make: Smart Instruments Company Pvt. Ltd., India) was employed to gauge the density (ρ) of the $CdIn_2Se_4$ ternary semiconducting compound. Fourier transform infrared (FTIR) spectroscopy (model: Spectrum GX FT-IR, make: PerkinElmer, USA) was effected at room temperature (RT) ($\simeq$300 K) in the wavenumber ($\bar{\nu}$) range of 4000–400 cm^{-1} to perceive the functional group/s (if any) extant in the synthesized $CdIn_2Se_4$ bulk.

3. Results and discussion

3.1. X-ray diffraction (XRD) analysis

The $CdIn_2Se_4$ ternary semiconducting compound's synthesis was investigated using room temperature (RT) ($\simeq$300 K) X-ray diffraction (XRD) analysis. Fig. 1 illustrates the powder X-ray diffractogram of the $CdIn_2Se_4$ ternary semiconducting compound with the histogram (in red) screening standard data (ICDD card 01-089-2388). The pragmatic diffraction pattern accords pleasingly with the standard ICDD data. The strong diffraction peak at 26.5277° 2θ along with the other major diffraction peaks at 21.5954° 34.4587°, 37.8671°, 44.0075°, and 52.1227° agreeing to the (111), (101), (201), (112), (202), and (113) reflection planes stretches the signature for the establishment of the untainted $CdIn_2Se_4$ system [ICDD card 01-089-2388]. High levels of crystallinity are opined by a potent X-ray diffraction (XRD) peak intensity and a modest full width at half maximum (FWHM) value in the synthesized $CdIn_2Se_4$ ternary semiconducting compound. Three phases of tetragonal $CdIn_2Se_4$ (α, β, and γ) are distinguished by their c/a ratio value. The c/a ratio is 1 in α-(phase), 2 in β-(phase), and 4 in γ-(phase) $CdIn_2Se_4$. Since the c/a ratio in the α-phase of tetragonal $CdIn_2Se_4$ is 1, giving the appearance that the system is cubic, it is also referred to as a pseudo-cubic crystal system. According to ICDD card 01-089-2388, the α-(phase) $CdIn_2Se_4$ ternary semiconducting compound has a single-phase tetragonal (pseudo-cubic) ($c \simeq a$) structure and crystallographic space group (SG) $P\bar{4}2m(111)$.[30] The most prevalent structure of $CdIn_2Se_4$ is tetragonal α-phase, where two Cd ions, one In ion, and one vacancy coordinate each cation tetrahedrally. The high-intensity mountaintops of X-ray diffraction (XRD), *i.e.*, (111), (201), (202), and (113), have been employed for exhaustive scrutiny throughout the study.

To learn the d-interplanar spacings, the diffraction angle (2θ) of each reflection is measured, and the protuberant Bragg's relation is applied (eqn (1)):[41]

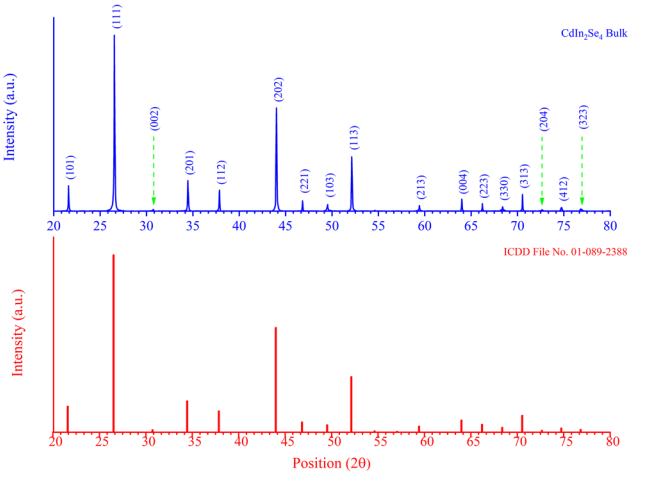

Fig. 1 X-ray diffractogram of the ternary semiconducting compound $CdIn_2Se_4$.

Table 2 d-Interplanar spacings, stacking faults (SF), and texture coefficients (C_i) for the ternary semiconducting compound $CdIn_2Se_4$

					d-interplanar spacing values (nm)				
h	k	l	2θ (°)	Intensity (a.u.)	Reported[a]	Calculated[b]	Calculated[c]	SF ($\times 10^{-3}$)	C_i
1	1	1	26.5277	100.0000	0.3357	0.3358	0.3359	1.0267	1.0003
2	0	1	34.4587	017.3729	0.2601	0.2601	0.2602	0.9057	0.9987
2	0	2	44.0075	058.7663	0.2056	0.2057	0.2057	0.7958	0.9997
1	1	3	52.1227	030.9344	0.1753	0.1754	0.1754	0.7300	1.0014

[a] ICDD card 01-089-2388. [b] X-ray diffraction (XRD) pattern of the bulk (using Bragg's law). [c] Bravais theory.

$$n\lambda = 2d\sin\theta \tag{1}$$

Table 2 equivalences the d-interplanar spacings found for each reflection to the facts found by Hahn *et al.*[42]

Stacking faults (SF) are defects in crystallography that designate the ineptness of crystallographic planes and are thus stared as planar defects (2D). The stacking fault (SF) morals of un-doped $CdIn_2Se_4$ for four intense peaks [(111), (201), (202), and (113)] are intended using eqn (2) and presented in Table 2,[43]

$$\mathrm{SF} = \frac{0.2533\beta}{(\tan\theta)^{1/2}} \tag{2}$$

In the above relation, β is the measure of full breadth/width at half maximum (FWHM) of the diffraction peak.

Exploiting eqn (3), one can discern the crystallites' preferred orientation along a crystal plane (hkl) by gauging the texture coefficient (C_i) of each X-ray diffraction (XRD) peak,[44]

$$C_i\sum_{i=1}^{N}\left(\frac{I_i}{I_{i0}}\right) = N\left(\frac{I_i}{I_{i0}}\right) \tag{3}$$

In this context, C_i denotes the texture coefficient of plane i, I_i denotes the leisurely integral intensity, I_{io} denotes the integral intensity of the reported data (ICDD powder diffraction pattern) of the comparable peak i, and N, which is equal to four (=4) in the current study, denotes the number of reflections in the X-ray diffraction (XRD) pattern utilized for analysis. The value of texture coefficient (C_i) is unity ($\simeq$1) for each reflection in the case of a capriciously oriented sample; grander than unity (>1), it designates the favored orientation of the crystallites in that specific direction.[45] The texture coefficient (C_i) of all four significant peaks [(111), (201), (202), and (113)] for the $CdIn_2Se_4$ ternary semiconducting compound are accessible in Table 2.

The degree of preferred orientation (Δ) of the $CdIn_2Se_4$ ternary semiconducting compound can be adjudicated by reckoning the standard deviation of all the texture coefficient (C_i) values using eqn (4):[44]

$$\Delta^2 N = \sum_{i=1}^{N}(C_i - C_{i0})^2 \tag{4}$$

C_{i0} is the texture coefficient (=1) in the overhead relation. Δ indicates the degree of preferred orientation of a sample; a zero ($\simeq$0) value of the degree of preferred orientation (Δ) acclaims that the material has utterly random orientation; a higher degree of preferred orientation (Δ) leads to amended preferential orientation. The value of the degree of preferred orientation (Δ) was found to be 9.6751×10^{-4} for the $CdIn_2Se_4$ ternary semiconducting compound.[46]

The Bravais theory determines the distance between the crystal planes, *i.e.*, d-interplanar spacing (d_{hkl}), to shed light on the synthesized material's growth. Based on his tactic, Bravais offers the relation $h_{hkl} \propto R_{hkl} \propto \frac{1}{d_{hkl}}$, where R_{hkl} is the growth rate of the plane. For a given set of cell parameters for the $CdIn_2Se_4$ crystal system (a, b, c, α, β, γ), the d-interplanar spacing (d_{hkl}) for four significant peaks [(111), (201), (202), and (113)] can be intended by using eqn (5):[47]

$$\frac{1}{d_{hkl}} = \sqrt{\frac{\frac{h}{a}\begin{vmatrix}\frac{h}{a} & \cos\gamma & \cos\beta\\ \frac{k}{b} & 1 & \cos\alpha\\ \frac{l}{c} & \cos\alpha & 1\end{vmatrix} + \frac{k}{b}\begin{vmatrix}1 & \frac{h}{a} & \cos\beta\\ \cos\gamma & \frac{k}{b} & \cos\alpha\\ \cos\beta & \frac{l}{c} & 1\end{vmatrix} + \frac{l}{c}\begin{vmatrix}1 & \cos\gamma & \frac{h}{a}\\ \cos\gamma & 1 & \frac{k}{b}\\ \cos\beta & \cos\alpha & \frac{l}{c}\end{vmatrix}}{\begin{vmatrix}1 & \cos\gamma & \cos\beta\\ \cos\gamma & 1 & \cos\alpha\\ \cos\beta & \cos\alpha & 1\end{vmatrix}}} \tag{5}$$

Table 3 Comparison of unit cell parameters ($a = b \simeq c$) and cell volume (V) for the ternary semiconducting compound $CdIn_2Se_4$

a (nm)	V (nm^3)	Reference
0.5810	0.1961	50
0.5815	0.1966	ICDD card 01-089-2388
0.5818	0.1969	Powder diffraction data[a]
0.5818	0.1969	N–R method (Section 4.3.1)[a]
0.5819	0.1970	51
0.5820	0.1969	48
0.5820	0.1971	52
0.5824	0.1975	53

[a] Current investigation.

As evident from Table 2, the calculated d-interplanar spacing (d_{hkl}) for four significant peaks of $CdIn_2Se_4$ confirms that d_{111} is the largest, inferring that h_{111} is the smallest, *i.e.*, the growth rate of the (111) plane R_{111} is the smallest according to Bravais theory.[47] The Bravais theory confirms the growth of $CdIn_2Se_4$'s (111) plane.[48]

Using the Miller indices for the prime (111) plane, the tetragonal crystal system's eqn (6) used to obtain the lattice constant (a) of the α-$CdIn_2Se_4$ ternary semiconducting compound,[44]

$$d^{-2} = a^{-2}(h^2 + k^2) + c^{-2}l^2 \quad (6)$$

The lattice parameter's (a) figured moral (in ascending order) is comparable to the datasets (Table 3). The tetragonal crystal system's relation $V = a^2c$ ($\simeq a^3$ for α-$CdIn_2Se_4$ ternary semiconducting compound) makes it possible to infer the unit cell volume (V) of the ternary semiconducting compound $CdIn_2Se_4$.[49]

Comparing ternary semiconducting compound $CdIn_2Se_4$'s unit cell parameter (a) to standard data reveals a 0.052% anomaly.

3.2. Rietveld refinement (RR)

The Rietveld refinement (RR) method in the FullProf suite was used to evaluate the X-ray diffraction (XRD) data to estimate $CdIn_2Se_4$'s thermal and structural parameters [J thoroughly. Rodriguez-Caravajal, Fullprof Version, 7.40]. The X-ray diffractogram of the ternary semiconducting compound $CdIn_2Se_4$ system following Rietveld refinement (RR) is shown in Fig. 2.

Rietveld refined data points and added structural factors were selected to define the backdrop during refining. The red solid circles epitomize the ternary semiconducting compound $CdIn_2Se_4$'s observed (experimental) diffractogram, and the black solid circles signify the pattern retrieved from Rietveld refinement (RR), the vertical bars designate the Bragg's position, and the bottommost line stipulates the difference between the observed and calculated profiles. The structural analysis defined peak shapes and full width at half maxima (FWHM) using a linear alliance of a Gaussian and a Lorentzian function (pseudo-Voigt) at various Bragg positions.

Fig. 3 denotes the polyhedron depiction of the ternary semiconducting compound $CdIn_2Se_4$'s unit cell with a tetragonal

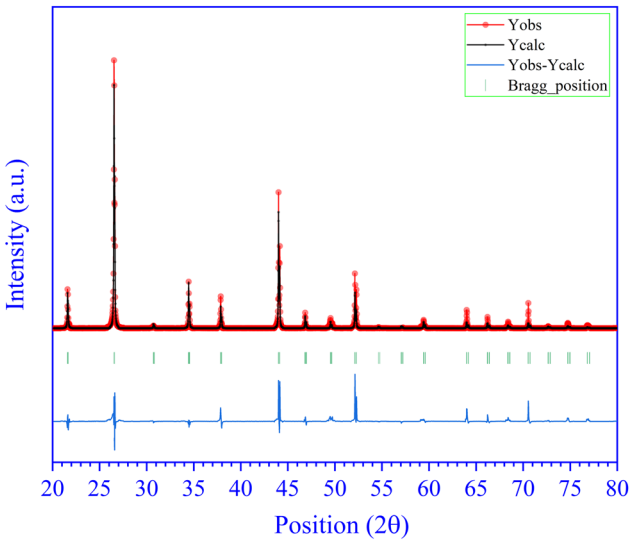

Fig. 2 Rietveld profile fitting of the ternary semiconducting compound $CdIn_2Se_4$.

structure formed by the VESTA program.[4] The ternary semiconducting compound $CdIn_2Se_4$ bulk system does not designate any impurity phase/s. It is apparent from the polyhedra unit cell that the $CdSe_4$ tetrahedra share corners with the eight corresponding $InSe_4$ tetrahedra that are formed by bonding Cd^{2+} to four equivalent Se^{2-} atoms. When In^{3+} is linked to four comparable Se^{2-} atoms, $InSe_4$ tetrahedra are created, which share corners with four $CdSe_4$ tetrahedra and corners with four $InSe_4$ tetrahedra. In a trigonal non-coplanar geometry, Se^{2-} is joined to one Cd^{2+} and two equivalent In^{3+} atoms.

Fig. 4a and b exemplify the electron density inside the ternary semiconducting compound $CdIn_2Se_4$ unit cell using the GFourier tool in the FullProf Package. The electron density was measured in electrons per cubic angstrom (e Å^{-3}). Bond distances and angles for the ternary semiconducting compound $CdIn_2Se_4$ system were calculated using the VESTA tool with the

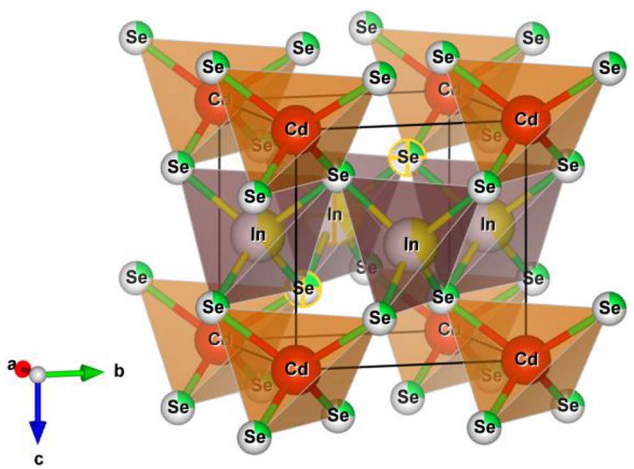

Fig. 3 Polyhedron representation of the tetragonal structure of the ternary semiconducting compound $CdIn_2Se_4$.

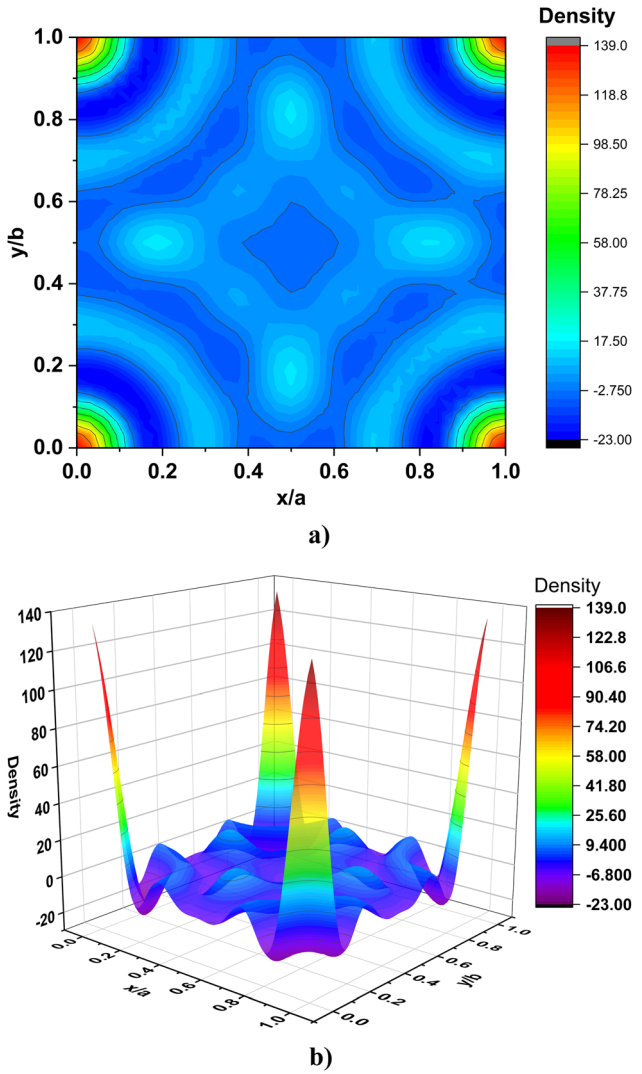

Fig. 4 (a) 2D, and (b) 3D electron density maps of individual atoms on the x–y ($z = 0$) plane in the unit cell of the ternary semiconducting compound $CdIn_2Se_4$.

X-ray diffraction (XRD) parameters obtained after structural refinement with FullProf, which was then used to produce a crystallographic information file (CIF).[54] Cd^{2+} cations lodge the Wycoff ($1a$) sites at (0, 0, 0), In^{3+} cations lodge at the Wycoff site $2f$ at two different positions $\left(\frac{1}{2}, 0, \frac{1}{2}\right)$ and $\left(0, \frac{1}{2}, \frac{1}{2}\right)$, respectively, whereas Se^{2-} anions lodge the Wycoff ($4n$) sites at four different positions (0.7279, 0.2720, 0.7636), (0.2720, 0.2720, 0.2363), (0.2720, 0.7279, 0.7636), and (0.7279, 0.7279, 0.2363) in the ternary semiconducting compound $CdIn_2Se_4$ system [ICDD card 01-089-2388].[30] The cell parameters (a, b, c, α, β, γ) and their error bars are resolute using a tetragonal structure with the $P\bar{4}2m(111)$ symmetry for the ternary semiconducting compound $CdIn_2Se_4$. Numerous reliability parameters such as Bragg's R-factor (R_B%), profile factor (R_p%), crystallographic factor (R_F%), weighted profile factor (R_{wp}%), expected profile factor (R_{exp}%), goodness of fit (S), chi^2 (χ^2%), crystal cell volume (V), and profile parameters (u, v, and w) for the ternary semiconducting compound $CdIn_2Se_4$ system are construed and presented in Table 4. The values in bracket designate error bars.

Table 4 System parameters of the ternary semiconducting compound $CdIn_2Se_4$

Parameters	Symbol/unit	Values
Cell parameters	$a = b$ (Å)	5.81385 (0)
	c (Å)	5.81536 (0)
	$\alpha = \beta = \gamma$	90.00°
Space group	SG	$P\bar{4}2m(111)$
Bragg's R-factor	R_B%	25.0
Profile factor	R_p%	24.9
Crystallographic factor	R_F%	22.2
Weighted profile factor	R_{wp}%	17.2
Expected profile factor	R_{exp}%	13.5
Goodness of fit	S	1.27
Chi^2	χ^2%	0.12
Crystal cell volume	V (Å^3)	196.564 (0.000)
Profile parameters	u	0.060332
	v	−0.026456
	w	0.037855

Electron density mapping is used to study the spreading of electron densities within the tetragonal cell to extricate between the atomic positions of the elements in a crystal's unit cell. The scattering electron density is approached using eqn (7) and the Fourier Transform of the geometrical structural factor $\rho(x, y, z)$ (electron density at a point x, y, z inside a unit cell volume V),[55]

$$\rho(x, y, z) \times V = \sum |F_{hkl}| \exp\{-2\pi i(hx + ky + lz - \alpha_{hkl})\} \quad (7)$$

The amplitude of the structure component is symbolized by F_{hkl}, while the phase angle of each Bragg reflection is symbolized by α_{hkl}. A two (2D)- or three (3D)-dimensional Fourier map was used to exemplify the electron scattering density $\rho(x, y, z)$. Typically, the contours in a two-dimensional (2D) Fourier plot portray the distribution of electron concentrations adjacent to each element in the solution. Elements housed in unit cells tend to be heavier when their electron density contours are thick and dense; a three-dimensional (3D) Fourier map encapsulates a network resembling chicken wire with a single electron density level. Fig. 4a demonstrates the two-dimensional (2D) Fourier electron density mapping of the cadmium (Cd), indium (In), and selenium (Se) atoms in the ternary semiconducting compound $CdIn_2Se_4$ unit cell on the x–y plane ($z = 0$). The electron distribution in the valence 4s and 3d orbitals might cause the contours around the cadmium (Cd). The silhouette in Fig. 4a displays the electron density levels with the coloured area surrounding cadmium (Cd), indium (In), and selenium (Se); on the contrary, the black line expresses the zero-level density contour. The three-dimensional (3D) Fourier density mapping of the cadmium (Cd), indium (In), and selenium (Se) elements in the ternary semiconducting compound $CdIn_2Se_4$ unit cell at $z = 0$ is shown in Fig. 4b.

Table 5 clearly presents the bond (interatomic) lengths, bond angles, and atom parameters (characteristics) of the ternary semiconducting compound $CdIn_2Se_4$.[29]

Table 5 Bond lengths, bond angles, and atomic parameters of the ternary semiconducting compound $CdIn_2Se_4$ (errors are enclosed in brackets)

Bond length (Å)		Bond angle (degree)	
Cd_1–Se_1	2.6248 (0)	Se_1–Cd_1–Se_1	116.8559 (0)
Cd_2–Se_2	2.6254 (0)	Se_2–Cd_2–Se_2	105.9128 (0)
Cd–Cd	5.8138 (0)	Cd_1–Se_1–In_1	104.6155 (0)
In–Se	2.5708 (0)	Cd_2–Se_2–In_2	104.5964 (0)
		Se_1–In_1–Se_1	106.7785 (0)
		Se_2–In_2–Se_2	117.9247 (0)
		Se_3–In_3–Se_3	104.0534 (0)

Atomic parameters

Atom	x	y	z	Occupancy	Multiplicity
Cd	0.00000 (0)	0.00000 (0)	0.00000 (0)	1.046 (0)	1
In_1	0.50000 (0)	0.0000 (0)	0.50000 (0)	0.868 (0)	2
In_2	0.0000 (0)	0.50000 (0)	0.50000 (0)	1.000 (0)	2
Se_1	0.72790 (0)	0.27200 (0)	0.76360 (0)	1.087 (0)	4
Se_2	0.27200 (0)	0.27200 (0)	0.23630 (0)	0.994 (0)	4
Se_3	0.27200 (0)	0.72790 (0)	0.76360 (0)	1.000 (0)	4
Se_4	0.72790 (0)	0.72790 (0)	0.23630 (0)	1.001 (0)	4

3.3. Microstructural parameter analysis

Inspecting the microstructural characteristics of the semiconducting material formerly used to create advanced technological devices is decisive. Several microstructural properties, including lattice parameters (a, b, and c), crystallite size (D), lattice strain (ε), root mean square strain (ε_{rms}), dislocation density (δ), lattice stress (σ) and energy density (u) can be inferred by examining the X-ray diffractogram of the ternary semiconducting compound $CdIn_2Se_4$.[56–58] Following the Gaussian and Lorentzian distribution functions, the peak shape corrects the full width at half maximum (FWHM). As a result of internal lattice stress (σ), lattice strain (ε) causes a unit cell's length to be stretched or compressed relative to its original dimension. Contingent on the crystallite size (D) and lattice strain (ε), Bragg's peak has diverse effects; crystallite size (D) and lattice strain (ε) influence peak width, whereas the intensity of the peak affects the diffraction angle (2θ) position. Diverse approaches were used in the present investigation to examine the ternary semiconducting compound $CdIn_2Se_4$'s microstructural parameters.

3.3.1. Nelson–Riley (N–R) method. It is possible to determine the lattice parameter (a) of the tetragonal α-phase $CdIn_2Se_4$ ternary semiconducting compound using the Nelson–Riley (N–R) technique (also referred to as the error function). The Nelson–Riley (N–R) graph was contrived between the calculated lattice parameters (a) from different planes [(111), (201), (202), and (113)] and the error function ($f(\theta)$) by employing eqn (8):[44]

$$2f(\theta) = \frac{\cos^2\theta}{\sin\theta} + \frac{\cos^2\theta}{\theta} \quad (8)$$

In the Nelson–Riley (N–R) plot (Fig. 5), the intercept was used to gauge the lattice parameter [Intercept = a ($\simeq c$)] of the tetragonal α-phase $CdIn_2Se_4$ ternary semiconducting compound, and the outcome is accessible in Table 3.

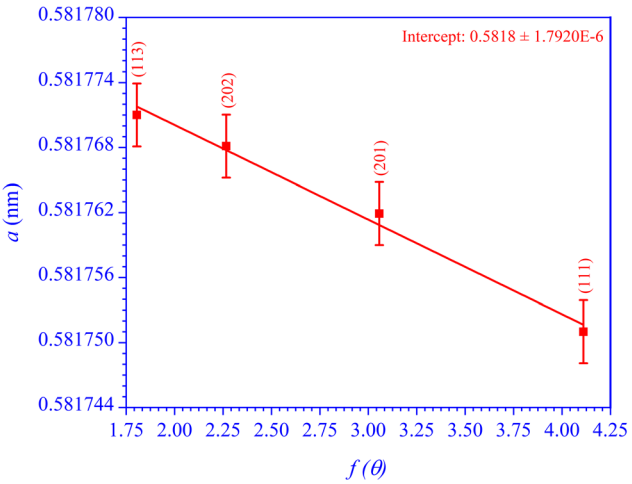

Fig. 5 N–R diagram of the ternary semiconducting compound $CdIn_2Se_4$.

3.3.2. Scherrer method. The crystallite size (D) of the tetragonal α-phase $CdIn_2Se_4$ ternary semiconducting compound can be estimated from the breadth/width of X-ray diffraction (XRD) lines using the Scherrer eqn (9):[56]

$$D\beta\cos\theta = K\lambda \quad (9)$$

The estimate of the crystallite size (D) is based on the default value of 0.9 for the Scherrer constant (K) since its exact value is unknown for the current material system ($CdIn_2Se_4$ ternary semiconducting compound). Re-arranging eqn (9), we obtained eqn (10):

$$\frac{1}{\beta} = \frac{D\cos\theta}{K\lambda} \quad (10)$$

The crystallite size (D) ($=K \times \lambda \times$ slope $= 1.3869 \times 10^{-10} \times$ slope) of the $CdIn_2Se_4$ ternary semiconducting compound was estimated from the Scherrer plot (Fig. 6a), and is presented in Table 6.

The Stokes–Wilson (S–W) eqn (11) was utilized to ascertain the lattice strain (ε) persuaded in the $CdIn_2Se_4$ ternary semiconducting compound as a result of crystal imperfection and disorder:[59]

$$\beta = 4\varepsilon\ \tan\ \theta \quad (11)$$

The middling lattice strain (ε) ($=0.25 \times$ slope) envisioned from the Stokes–Wilson (S–W) plot (Fig. 6b), for the $CdIn_2Se_4$ ternary semiconducting compound is accessible in Table 6.

The $CdIn_2Se_4$ ternary semiconducting compound's root mean square strain (ε_{rms}) was determined using the Stocks–Wilson (S–W) eqn (12) along each crystallographic plane [(111), (201), (202), and (113)]:[59]

$$\varepsilon_{rms} = \sqrt{\frac{2}{\pi}}\varepsilon \quad (12)$$

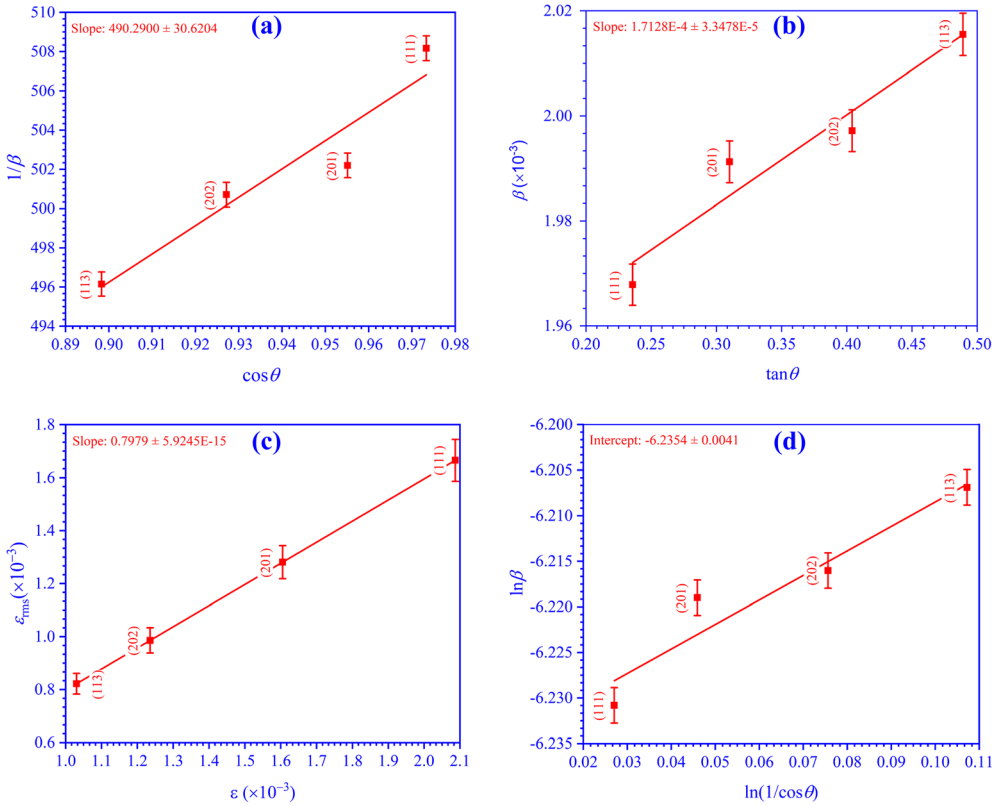

Fig. 6 (a) Sherrer, (b) S–W, (c) ε_{rms}–ε, and (d) Monshi plots for the ternary semiconducting compound $CdIn_2Se_4$.

Table 6 Microstructural parameters of the ternary semiconducting compound $CdIn_2Se_4$

Method		Microstructural parameters			
		D (nm)	ε ($\times10^{-3}$)	σ ($\times10^{6}$) (Pa)	u ($\times10^{3}$) (J m^{-3})
Scherrer		67.9983	0.0428	-	-
Monshi		70.8019	—	-	-
W–H	UDM	66.0429	−0.1304	-	-
	USDM	69.0000	—	−2.8496	-
	UDEDM	68.3202	—	-	0.1860
SSP		70.7602	−0.1811	-	-
H–W		78.6733	−1.1750	-	-

The fact that the data points are lying straight with an abscissa at an angle of 38.5864° is clear from Fig. 6c, which shows that the root mean square strain (ε_{rms}) varies linearly with lattice strain (ε), demonstrating that the lattice planes' crystallographic direction is consistent.[60]

3.3.3. Monshi method. As the diffraction angle (2θ) values increased, Rabiei *et al.*[61] testified that Scherrer's equation raised the projected nanocrystalline sizes. Eqn (13) perfectly captures how Monshi modified Sherrer's original formula:[62]

$$\ln \beta = \ln\left(\frac{K\lambda}{D}\right) + \ln\left(\frac{1}{\cos\theta}\right) \quad (13)$$

The crystallite size (D) ($=K \times \lambda \times e^{-intercept} = 1.3869 \times 10^{-10} \times e^{-intercept}$) for the $CdIn_2Se_4$ ternary semiconducting compound was estimated from Fig. 6d, and is presented in Table 6.

3.3.4. Williamson–Smallman's (W–S) method. The dislocation density (δ) for the ternary semiconducting compound $CdIn_2Se_4$ can be intended by substituting the value of crystallite size (D) attained from Scherrer's way into eqn (14):

$$\delta = \frac{1}{D^2} \quad (14)$$

Williamson–Smallman's (W–S) method deduces $\simeq 0.2163 \times 10^{-3}$ lines nm^{-2} (ref. 56) dislocation density (δ) for the ternary semiconducting compound $CdIn_2Se_4$.

3.3.5. Williamson–Hall (W–H) method. The crystallite size (D) and lattice strain (ε) of the tetragonal α-phase $CdIn_2Se_4$ ternary semiconducting compound were determined using the Scherrer and Monshi methods and the Stokes–Wilson (S–W) method, respectively, while considering the broadening of the breadth/width of X-ray diffraction (XRD) lines. However, neither technique could visualize the effects of powder defects on the determination of crystallite size (D) or lattice strain (ε). Given that the broadening of the breadth/width of X-ray diffraction (XRD) lines may be caused by a Gaussian and/or Lorentzian function, the modified Williamson–Hall (W–H) equation can be used to derive uniform deformation (UDM), uniform stress deformation (USDM), and uniform deformation energy density

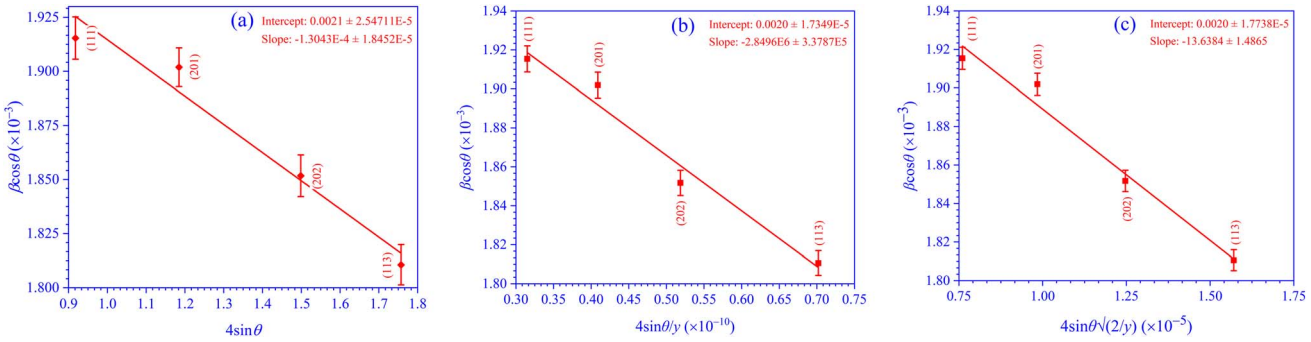

Fig. 7 W–H plots: (a) UDM, (b) USDM, and (c) UDEDM for the ternary semiconducting compound $CdIn_2Se_4$.

(UDEDM) models; which lets one estimate the crystallite size (D), lattice strain (ε), lattice stress (σ), and energy density (u) values of the ternary semiconducting compound $CdIn_2Se_4$.[63]

3.3.5.1. Uniform deformation model (UDM) method. Due to crystal defects and distortion, the $CdIn_2Se_4$ ternary semiconducting compound's crystallite size (D) and lattice strain (ε) can be estimated using the uniform deformation model (UDM) approach, which is derived by modifying the Williamson–Hall (W–H) eqn (15):[64]

$$\beta \cos\theta = \frac{K\lambda}{D} + 4\varepsilon \sin\theta \tag{15}$$

Table 6 provides the crystallite size (D) ($=K \times \lambda \times \text{intercept}^{-1} = 1.3869 \times 10^{-10} \times \text{intercept}^{-1}$) and lattice strain ($\varepsilon$) (=slope) obtained using Fig. 7a as a straight-line plot.

3.3.5.2. Uniform stress deformation model (USDM) method. The Williamson–Hall (W–H) equation needs to be modified to consider the characteristics of an anisotropic crystal because the uniform deformation model (UDM) approach has the flaw of assuming an isotropic, homogeneous crystal, which is not the case in the actual crystallographic system. Hooke's law states that lattice strain (ε) and lattice stress (σ) are linearly related within the elastic limit, resulting in lattice stress (σ) = lattice strain (ε) × Young's modulus (y). By replacing the lattice strain (ε) by $\frac{\text{lattice stress } (\sigma)}{\text{Young's modulus } (y)}$ into eqn (15), we obtained eqn (16):[63]

$$\beta \cos\theta = \frac{K\lambda}{D} + \frac{4\sigma \sin\theta}{y} \tag{16}$$

To estimate the crystallite size (D) and lattice stress (σ) of the ternary semiconducting compound $CdIn_2Se_4$, eqn (16) requires the values of Young's modulus (y) for each (hkl) plane (y_{hkl}) [(111), (201), (202), and (113)].

For the tetragonal crystal system, eqn (17) relates Young's modulus (y) for each (hkl) plane (y_{hkl}) with elastic compliance constants (S_{ij}) and stiffness constants (C_{ij}):[5]

$$\frac{1}{y_{hkl}} = \frac{l^4(S_{33} - 2S_{13} - S_{44}) + h^2k^2(2S_{12} + S_{66})}{\left(h^2 + k^2 + l^2\right)^2} + \frac{S_{11}\left(h^2 + k^2\right) + l^2(2S_{13} + S_{44})}{\left(h^2 + k^2 + l^2\right)} \tag{17}$$

Young's modulus (y_{hkl}) for preferred orientations (111), (201), (202), and (113) were determined to be 29.1266, 28.9776, 28.8912, and 25.0328 GPa, respectively, for the ternary semiconducting compound $CdIn_2Se_4$ by entering values of various elastic compliance constants (S_{ij}) into eqn (17).[4] By substituting Young's modulus (y_{hkl}) values derived by using eqn (17) into eqn (16) and plotting Fig. 7b, the plot's straight line derives the crystallite size (D) ($=K \times \lambda \times \text{intercept}^{-1} = 1.3869 \times 10^{-10} \times \text{intercept}^{-1}$) and lattice stress ($\sigma$) (=slope) for ternary semiconducting compound $CdIn_2Se_4$. The extracted values are presented in Table 6.

3.3.5.3. Uniform deformation energy density model (UDEDM) method. As required by Hooke's law, the uniform stress deformation model (USDM) assumes a linear relationship between the lattice strain (ε) and the lattice stress (σ). However, imperfections such as dislocations and agglomerations make accounting for real crystals' isotropic nature and linear proportionality impossible. In particular, the uniform anisotropic deformation of the lattice in all crystallographic directions and the origin of deformation, which is characterized as the deformation energy density (u) $\left(= \frac{\varepsilon^2 y}{2} \Rightarrow \varepsilon = \sqrt{\frac{2u}{y}}\right)$,[63] are considered by the uniform deformation energy density model (UDEDM) technique. By substituting $\varepsilon = \sqrt{\frac{2u}{y}}$ into eqn (15), we obtained eqn (18):

$$\beta \cos\theta = \frac{K\lambda}{D} + 4 \sin\theta \sqrt{\frac{2u}{y}} \tag{18}$$

Table 6 presents the crystallite size (D) ($=K \times \lambda \times \text{intercept}^{-1} = 1.3869 \times 10^{-10} \times \text{intercept}^{-1}$) and energy density ($u$) ($=\text{slope}^2$) of the ternary semiconducting compound $CdIn_2Se_4$, estimated from the straight-line plot in Fig. 7c.

3.3.6. Size–strain plot (SSP) method. The Williamson–Hall (W–H) critique posits that the broadening of the peak is a feature of the diffraction angle (2θ), resulting from the additive effects of the crystallite size (D) and lattice strain (ε) stimulated broadening. The size-strain plot (SSP) approach considers the X-ray diffraction (XRD) line analysis to be a combination of Lorentzian and Gaussian functions, the former addressing broadening due to crystallite size (D) and the

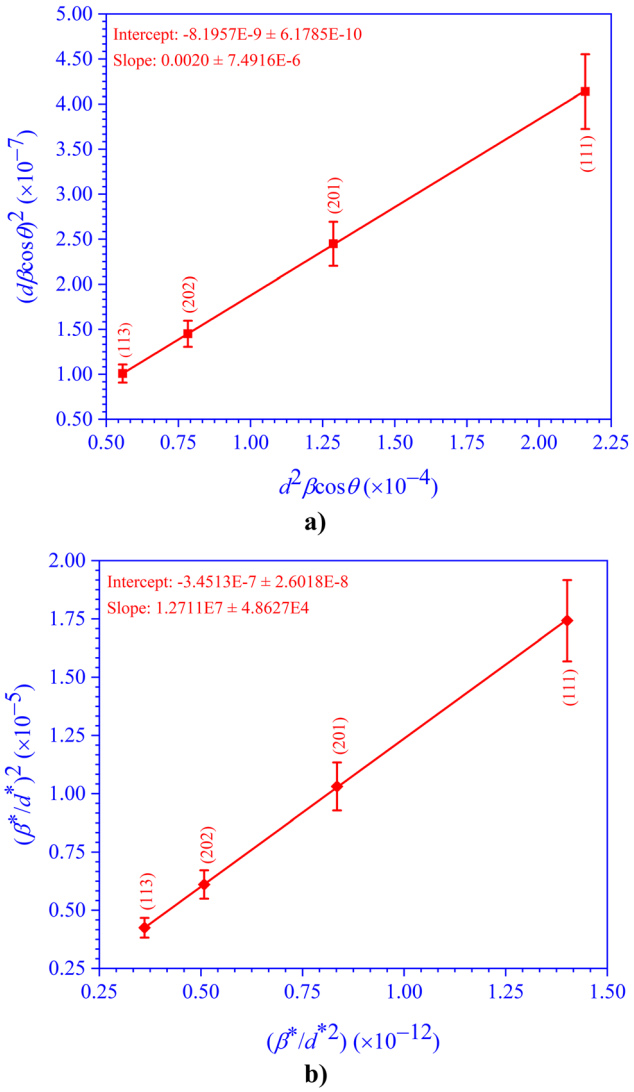

Fig. 8 (a) SSP and (b) H–W plots for the ternary semiconducting compound $CdIn_2Se_4$.

latter to lattice strain (ε). The size-strain plot (SSP) method was employed to estimate the crystallite size (D) and lattice strain (ε) of the ternary semiconducting compound $CdIn_2Se_4$ using eqn (19), as displayed in Fig. 8a:[65]

$$(d\beta\cos\theta)^2 = \frac{K\lambda}{D}\left(d^2\beta\cos\theta\right) + \frac{\varepsilon^2}{4} \quad (19)$$

The plot's linear fitting estimates crystallite size (D) ($=K \times \lambda \times \text{slope}^{-1} = 1.3869 \times 10^{-10} \times \text{slope}^{-1}$) and lattice strain ($\varepsilon$) ($= 2 \times \sqrt{\text{intercept}}$) for the ternary semiconducting compound $CdIn_2Se_4$. The results are accessible in Table 6.

3.3.7. Halder–Wagner (H–W) method. Given that the mid-peak area and the X-ray diffraction (XRD) peak's tail could not be mapped using the Gaussian and Lorentzian functions, respectively, the X-ray diffraction (XRD) peak width assumption in the size-strain plot (SSP) technique does not hold. To disprove the assumption made by the Halder–Wagner (H–W) analysis that peak broadening is the Voigt function, the convolution of Gaussian and Lorentzian functions is employed. Eqn (20) shows the relationship between the crystallite size (D) and the lattice strain (ε) as they relate to the Halder–Wagner (H–W) method,[66]

$$\frac{\beta^2\cos^2\theta}{4\sin^2\theta} = \frac{\lambda}{4D}\left(\frac{\beta\cos\theta}{\sin^2\theta}\right) + \frac{\varepsilon^2}{4} \quad (20)$$

The slope shown in Fig. 8b as a straight-line estimates crystallite size (D) ($=\text{slope}^{-1}$), whereas the intercept stretches lattice strain (ε) ($= 2 \times \sqrt{\text{intercept}}$) of the ternary semiconducting compound $CdIn_2Se_4$. The upshots are accessible in Table 6.

Consistency exists between the findings for the various methods' estimated crystallite size (D) and lattice strain (ε) virtues for the ternary semiconducting compound $CdIn_2Se_4$. The negative values of lattice strain (ε) and lattice stress (σ) for ternary semiconducting compound $CdIn_2Se_4$ indicate compressive lattice strain (ε) and lattice stress (σ) for the ternary semiconducting compound $CdIn_2Se_4$, which originates from the assertion of equal and opposing forces that cause a shrinking of the crystalline structure.[67,68]

3.3.8. Elastic modulus. The bulk modulus (B_H) measures the resistance of a material to the volume change, the shear modulus (G_H) measures the resistance of a material to a shape change, Young's modulus (y) relates tensile stress to tensile strain, which is often employed to measure the solid's stiffness, and the Poisson's ratio (ν) relates the negative morals of the transverse strain to the longitudinal strain.[69] The tetragonal ternary semiconducting compound $CdIn_2Se_4$ is evaluated for its bulk modulus (B_H), shear modulus (G_H), Young's modulus (y), and Poisson's ratio (ν).[27,28]

3.3.8.1. Bulk modulus (B_H). Voigt–Reuss (V–R) methods use eqn (21) and (22) to create a link between the elastic modulus (B_V and B_R) and elastic stiffness constants (C_{ij}) for tetragonal symmetric crystals:[70]

$$9B_V = 2(C_{11} + C_{12}) + C_{33} + 4C_{13} \quad (21)$$

$$B_R(C_{11} + C_{12} + 2C_{33} - 4C_{13}) = (C_{11} + C_{12})C_{33} - 2C_{13}^2 \quad (22)$$

The ternary semiconducting compound $CdIn_2Se_4$'s bulk modulus (B_H) value was found to be 40.7787 Gpa[29] by substituting B_V (=41.9676 GPa) and B_R (=39.5899 GPa) values obtained from eqn (21) and (22) into eqn (23):[70]

$$2B_H = B_R + B_V \quad (23)$$

The high bulk modulus (B_H) of α-phase $CdIn_2Se_4$ (40.7787 GPa) in comparison to β-phase $CdIn_2Se_4$ (17.6750 GPa) suggests that the compressibility of α-phase $CdIn_2Se_4$ is lower, resulting in small volume changes at high pressure, making it appropriate for piezoelectric applications.

3.3.8.2. Shear modulus (G_H). In tetragonal symmetric crystals, the Voigt–Reuss (V–R) techniques use eqn (24) and (25) to

create a link between the upper and lower bounds for the shear modulus (G_v and G_R) and elastic stiffness constants (C_{ij}),[70]

$$15G_V = 2C_{11} - C_{12} - 2C_{13} + C_{33} + 6C_{44} + 3C_{66} \quad (24)$$

$$\frac{5}{G_R} = \frac{6B_V}{(C_{11} + C_{12})C_{33} - 2C_{13}^2} + \frac{2}{C_{11} - C_{12}} + \frac{2}{C_{44}} + \frac{1}{C_{66}} \quad (25)$$

The ternary semiconducting compound $CdIn_2Se_4$'s shear modulus (G_H) value was found to be 15.5735 GPa[29] by substituting G_V (=17.1652 GPa) and G_R (=13.9817 GPa) values obtained from eqn (24) and (25) into eqn (26):[70]

$$2G_H = G_R + G_V \quad (26)$$

The high shear modulus of α-phase $CdIn_2Se_4$ (15.5735 GPa), in comparison to β-phase $CdIn_2Se_4$ (14.4220 GPa), indicates that α-$CdIn_2Se_4$ has higher retention and resistance to deformation than β-phase $CdIn_2Se_4$, which further demonstrates its significant employability in the manufacture of piezoelectric devices.

3.3.8.3. Young's modulus (y) and Poisson's ratio (ν). Young's modulus (y) for the ternary semiconducting compound $CdIn_2Se_4$ was found to be 41.4445 GPa[29] by substituting the values of bulk modulus (B_H) and shear modulus (G_H) into eqn (27):[70]

$$y(3B_H + G_H) = 9B_HG_H \quad (27)$$

The larger the value of Young's modulus (y), the stiffer the material.[69]

By placing the values of bulk modulus (B_H) and Young's modulus (y) in eqn (28),[38] Poisson's ratio (ν) for the ternary semiconducting compound $CdIn_2Se_4$ was determined to be 0.3306:[29]

$$6\nu B_H = 3B_H - y \quad (28)$$

Poisson's ratio (ν) usually represents the stability of the material against shear deformation, and its value ranges typically between −1.0 and 0.5 for a stable and linear elastic solid material; a more significant value of Poisson's ratio (ν) indicates that a solid has a good plasticity.

To determine whether a synthesized material is brittle (covalent) or ductile (ionic), the numerical values of Poisson's ratio (ν), Pugh's ratio, the ratio of semiconducting compound's bulk modulus (B_H) to shear modulus (G_H) (*i.e.* $\frac{B_H}{G_H}$), and Cauchy pressure (=$C_{12} - C_{44}$) were utilized. If conditions $\nu > 0.26$, $\frac{G_H}{B_H} < 0.57$, and the positive value of Cauchy pressure is satisfied, a solid is ductile (ionic); otherwise, it is brittle (covalent).[38] The ternary semiconducting compound α-$CdIn_2Se_4$'s ductile (ionic) nature can be confirmed by observing a Poisson ratio (ν) of 0.3306, Pugh's ratio of 2.6185, and a Cauchy pressure of +20.7867 GPa. β-$CdIn_2Se_4$ exhibits a brittle (covalent) character in contrast to α-$CdIn_2Se_4$.[29] As ductile materials have strong damage tolerance qualities, α-phase $CdIn_2Se_4$ is a promising contender for piezoelectric applications.

Hardness, an important mechanical property of a material, can be predictable by a Vickers hardness (H_V) (theoretical) model using eqn (29):[38]

$$\frac{H_V + 3}{2} = \left(\frac{G_H^3}{B_H^2}\right)^{0.585} \quad (29)$$

The value of H_V was found to be 5.9492×10^5 for the ternary semiconducting compound $CdIn_2Se_4$.

3.3.8.4. Elastic anisotropy. Phase transitions, precipitation, dislocation dynamics, anisotropic plastic deformation, crack behavior, and other mechanical and physical properties of materials all depend on elastic anisotropy. Random crystals are known to have anisotropic elastic properties; consequently, measuring the crystals' elastic anisotropy is necessary since precise anisotropy characterization is essential for practical applications of any material. Eqn (30)–(32) can be used to determine the universal elastic anisotropic index (A^U), percent compressible anisotropy (A_{comp}), and percent shear anisotropy (A_{shear}), which are used to characterize the elastic anisotropy of solids. For the ternary semiconducting compound $CdIn_2Se_4$, the values were found to be 1.1985, 2.9153%, and 10.2211%, respectively,[38]

$$A^U = 5\frac{G_V}{G_R} + \frac{B_V}{B_R} - 6 \quad (30)$$

$$A_{comp} = \frac{B_V - B_R}{B_V + B_R} \times 100\% \quad (31)$$

$$A_{shear} = \frac{G_V - G_R}{G_V + G_R} \times 100\% \quad (32)$$

Additionally, shear anisotropic factors, A_1, A_2, and A_3, of the tetragonal ternary semiconducting compound $CdIn_2Se_4$ were determined using eqn (33)–(35) to be 2.3048, 3.3005, and 2.8479, respectively,[69]

$$A_1(C_{11}C_{33} - C_{13}^2) = C_{44}(C_{11} + C_{33} + 2C_{13}) \quad (33)$$

$$A_2\left[\left(C_{66} + \frac{C_{11} + C_{12}}{2}\right)C_{33} - 2C_{13}^2\right] = C_{44}\left(C_{66} + \frac{C_{11} + C_{12}}{2} + C_{33} + 2C_{13}\right) \quad (34)$$

$$A_3(C_{11} - C_{22}) = 2C_{66} \quad (35)$$

The existence of elastic anisotropy in the ternary semiconducting compound $CdIn_2Se_4$ is demonstrated by the fact that its elastic anisotropic parameters do not satisfy the following two conditions: (1) $A^U = A_{comp} = A_{shear} = 0$ and (2) $A_1 = A_2 = A_3 = 1$.[69]

3.3.9. Melting temperature T_m. The melting temperature (T_m) of a material is an estimate of the temperature at which it can be used without suffering from significant oxidation, structural distortion, or chemical change; using eqn (36), the melting temperature (T_m) of the ternary semiconducting compound $CdIn_2Se_4$ was found to be 598.4678 ± 300 K,[71]

$$T_m = 354\ \text{K} + \left(\frac{1.5\ \text{K}}{10^9\ \text{Pa}}\right)(2C_{11} + C_{33}) \pm 300\ \text{K} \quad (36)$$

3.3.10. Debye temperature (θ_D). By using Navier's relations,[72] the transverse sound velocity (v_t) (also known as shear wave velocity (v_s)), $v_t^2\rho = G_H$, for the ternary semiconducting compound $CdIn_2Se_4$ was found to be 1.6749 km s^{-1} [refer to Section 4.5 for ternary semiconducting compound $CdIn_2Se_4$' density (ρ) value],[70] and the longitudinal sound velocity (v_l) (also known as compressional wave velocity (v_p)), $v_l = \sqrt{\frac{3B_H + 4G_H}{3\rho}}$, for the ternary semiconducting compound $CdIn_2Se_4$ is 3.3296 km s^{-1}.[27,28,70] The average wave velocity (v_m) for the ternary semiconducting compound $CdIn_2Se_4$ was found to be 1.8783 km s^{-1} obtainable by utilizing the relation $v_m = \left[\frac{1}{3}\left(\frac{2}{v_t^3} + \frac{1}{v_l^3}\right)\right]^{-1/3}$.[70]

An important characteristic that relates to specific heat and melting point is the Debye temperature (θ_D), the temperature at whi'h a crystal's maximum vibration mode occurs. The Debye temperature (θ_D) can be deduced by employing eqn (37):[38]

$$\theta_D = \frac{h}{k_B}\left[\frac{3n}{4\pi}\left(\frac{N_A\rho}{M}\right)\right]^{1/3} v_m \quad (37)$$

In the above relation, h is the Planck constant ($\simeq 6.6262 \times 10^{-34}$ J s), n is the atom number per formula unit of the $CdIn_2Se_4$ ternary semiconducting compound (=7), N_A' is Avogadro's number ($\simeq 6.0224 \times 10^{23}$ mol^{-1}), ρ is the density of $CdIn_2Se_4$ [refer to Section 4.5 for ternary semiconducting compound $CdIn_2Se_4$' density (ρ) value], k_B is the Boltzmann constant ($\simeq 1.3807 \times 10^{-23}$ J K^{-1}), M is the molecular weight of ternary semiconducting compound $CdIn_2Se_4$ ($\simeq 0.6579$ kg mol^{-1}), and v_m is the average wave velocity. For the ternary semiconducting compound $CdIn_2Se_4$, the Debye temperature (θ_D) was found to be $\simeq 183.9084$ K.[29] The relatively low value of the Debye temperature (θ_D) ($\simeq 183.9084$ K) implies a relatively weak chemical bonding strength in the ternary semiconducting compound $CdIn_2Se_4$, which may result in relatively low hardness (5.9492×10^5).[69] The mechanical characteristics of the ternary semiconducting compounds α-$CdIn_2Se_4$ and β-$CdIn_2Se_4$ are compared in Table 7. The authors used β-$CdIn_2Se_4$ as the mechanical properties of α-$CdIn_2Se_4$ have not yet been published.

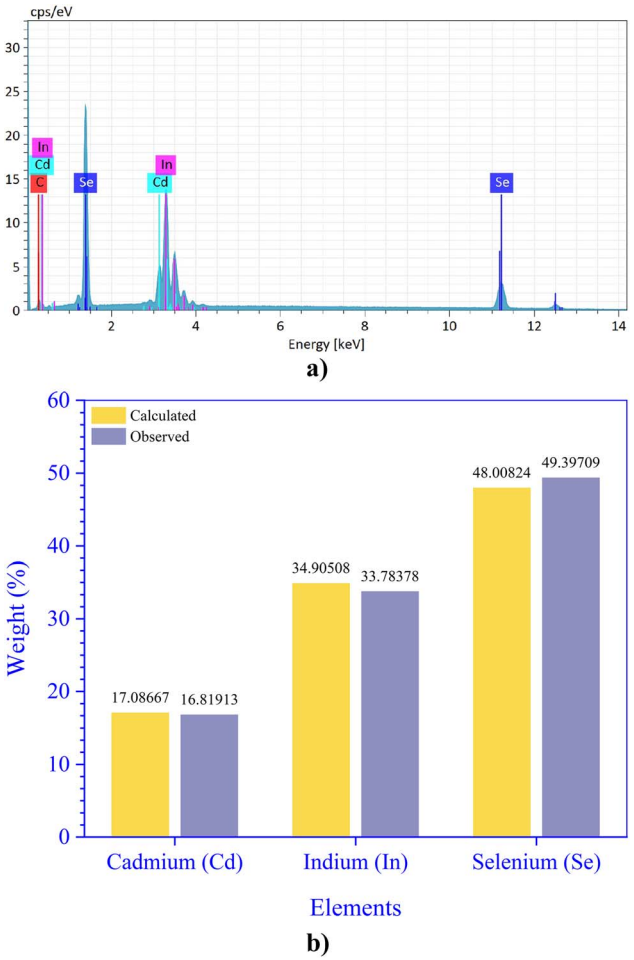

Fig. 9 (a) EDAX spectra of the ternary semiconducting compound $CdIn_2Se_4$. (b) Bar graph showing the calculated and observed weight percentages of Cd, In, and Se.

Table 7 Comparison of the mechanical properties of the ternary semiconducting compound $CdIn_2Se_4$

Mechanical properties	α-$CdIn_2Se_4$	β-$CdIn_2Se_4$ (ref. 29)
Bulk modulus (B_H) (GPa)	40.7787	17.6750
Shear modulus (G_H) (GPa)	15.5735	14.4220
Young's modulus (y) (GPa)	41.4445	33.9660
Poisson's ratio (ν)	0.3306	0.1800
Pugh's ratio	2.6185	1.2300
Cauchy pressure (GPa)	+20.7867	−09.3980
Elastic anisotropy: universal elastic anisotropic index (A^U)	1.1985	—
Elastic anisotropy: percent compressible anisotropy (A_{comp}) (%)	2.9153	—
Elastic anisotropy: percent shear anisotropy (A_{shear}) (%)	10.2211	—
Melting temperature (T_m) (K)	598.4678 ± 300	484.4300 ± 300
Transverse sound velocity (v_t) (km s^{-1})	1.6749	0.0002
Longitudinal sound velocity (v_l) (km s^{-1})	3.3296	0.0003
Average wave velocity (v_m) (km s^{-1})	1.8783	—
Debye temperature (θ_D) (K)	183.9084	172.9490

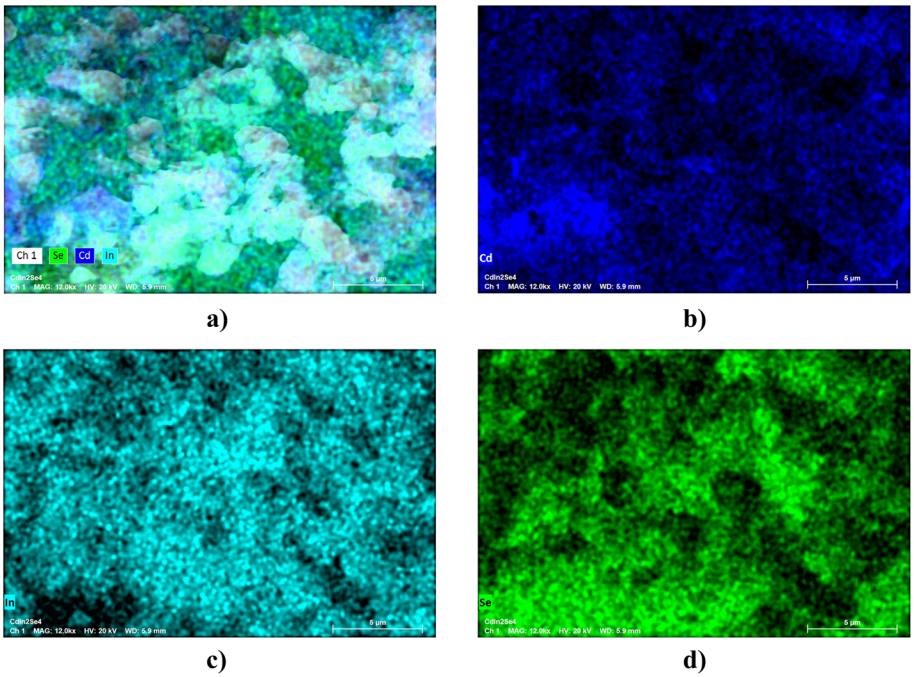

Fig. 10 Elemental mapping of the ternary semiconducting compound $CdIn_2Se_4$.

3.4. Energy-dispersive analysis of X-rays (EDAX)

After grinding the ternary semiconducting compound $CdIn_2Se_4$ into a fine powder, it was positioned on a specimen holder for scrutiny by energy-dispersive analysis using an X-ray (EDAX) instrument. First, the ingot was scrutinized by gross analysis, which involved scanning different specimen areas. Next, different points from the specimen were randomly chosen and examined. The ternary semiconducting compound $CdIn_2Se_4$'s energy-dispersive analysis of X-rays (EDAX), as shown in Fig. 9a and b, makes it evident that the ingot did not exhibit any discernible variation in the stoichiometric constituents of the elements, indicating that the ingot is homogeneous and stoichiometric. The empirical formula $CdIn_2Se_4$ has a stoichiometric weight percentage of $Cd_{17.09}In_{34.91}Se_{48.01}$, whereas the observed weight percentage is $Cd_{16.82}In_{33.78}Se_{49.40}$. The energy-dispersive analysis of X-ray (EDAX) spectra show a 1.5658 wt% deviation in cadmium (Cd), 3.2124 in indium (In), and 2.8929 in selenium (Se) when equated to their stoichiometric weight percentage.[4,48]

Fig. 10a displays the co-occurrence of all three elements. Fig. 10b–d show separate cadmium (Cd), indium (In), and selenium (Se) distributions, respectively. Cadmium (Cd), indium (In), and selenium (Se) are visualized on an elemental map with three distinct colours, dark blue (hexadecimal colour #000096; RGB values of R: 0, G: 0, B: 150, CMYK values of C: 1, M: 1, Y: 0, K: 0.41), cyan (hexadecimal colour #13CDE8; RGB values of R: 19, G: 205, B: 232, CMYK values of C: 0.92, M: 0.12, Y: 0, K: 0.09), and green (hexadecimal colour #37DC2D; RGB values of R: 55, G: 220, B: 45, CMYK values of C: 0.75, M: 0, Y: 0.80, K: 0.14); each of the three elements' numbers and colours indicate their relative concentrations.

3.5. Density measurement (ρ)

The ternary semiconducting compound $CdIn_2Se_4$ was measured for density (ρ) using a densitometer (pycnometer), and the outcomes propose that the lump is undeviating throughout its surface; the study's average density (ρ) value of 5551.2204 kg m^{-3} favours with the attested value [ICDD card 01-089-2388].[29,50]

3.6. Fourier transform infrared (FTIR) spectroscopy

Fig. 11 displays the room-temperature (RT) ($\simeq$300 K)-recorded Fourier transform infrared (FTIR) spectra of the ternary

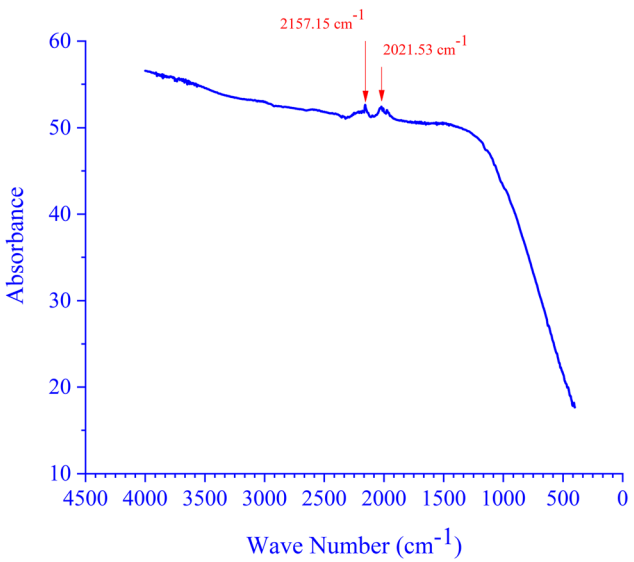

Fig. 11 FTIR spectra of the ternary semiconducting compound $CdIn_2Se_4$.

semiconducting compound $CdIn_2Se_4$. In synthesizing the ternary semiconducting compound $CdIn_2Se_4$, only 5 N (99.999%) pure cadmium (Cd), indium (In), and selenium (Se) were employed; no other chemicals or chemical routes were used. A peak perceived at a wavenumber ($\bar{\nu}$) of 2021.53 cm^{-1} can be assigned to the stretching N=C=S functional group and isothiocyanate class. A peak realized at a wavenumber ($\bar{\nu}$) of 2157.15 cm^{-1} can be assigned to the stretching S–C≡N functional group and thiocyanate class and/or stretching N=N=N functional group and azide class. The absorption peaks due to N=C=S, S–C≡N, and/or N=N=N functional group/s habitually display stout absorption edge in the spectra if existing in the synthesized ternary semiconducting compound $CdIn_2Se_4$. The absorption edges are evident from the Fourier transform infrared (FTIR) spectra of the ternary semiconducting compound $CdIn_2Se_4$ at 2021.53 cm^{-1} and 2157.15 cm^{-1} wavenumbers ($\bar{\nu}$), but they are feeble; henceforth, the synthesized ternary semiconducting compound $CdIn_2Se_4$ is untainted and free from any functional group.[21,73]

4. Conclusions

$CdIn_2Se_4$ belongs to the II–III_2–VI_4 family. The elastic constants for α-$CdIn_2Se_4$ were determined using the CASTEP module in the DFT framework under the PBE-GGA approach. $CdIn_2Se_4$ was created by melting 5 N pure stoichiometric amounts of Cd, In, and Se in a microcontroller-based controlled high-temperature rotary furnace. The crystal structure and phase purity of the synthesized $CdIn_2Se_4$ compound were investigated by XRD. Significant levels of crystallinity were demonstrated by its modest FWHM of the diffraction peak value and strong XRD peak intensity. The X-ray diffractogram peaks of $CdIn_2Se_4$ were recognized, indexed, and perfectly mapped with ICDD card 01-089-2388. The compound has the crystallographic space group (SG) $P\bar{4}2m$(111) and a single-phase pseudo-cubic α-phase tetragonal ($c \simeq a$) structure. For the most critical XRD peak (111), the stacking fault (SF) value of $CdIn_2Se_4$ was determined to be 1.0267×10^{-3}. The texture coefficient (C_i) of the XRD peaks of $CdIn_2Se_4$ were measured for the preferred orientations of the crystallites along a crystal plane (hkl), and the result was unity. $CdIn_2Se_4$ has a degree of preferred orientation (Δ) of 9.6751×10^{-4}. The Bravais theory determines the d-interplanar spacings (d_{hkl}) to shed light on the growth of the synthesized $CdIn_2Se_4$ compound, which enables the inference of the significance of the (111) plane of $CdIn_2Se_4$. Using Miller indices for the prime (111) plane, the lattice constant (a) of $CdIn_2Se_4$ is $\simeq$0.5818 nm, resulting in a cell volume of $\simeq$0.1969 nm^3. The Rietveld refinement (RR) in the Fullprof suite was used to evaluate the XRD data to estimate the thermal and structural parameters of $CdIn_2Se_4$ with a chi^2 value $\simeq$0.12. Several of the $CdIn_2Se_4$'s microstructural characteristics have been identified. According to the N–R method, the lattice parameter (a) of $CdIn_2Se_4$ is $\simeq 0.5817 \pm 0.0007$ nm. The size of the crystallite (D) was determined by the Scherrer, Monshi, W–H, SSP, and H–W methods to be $\simeq 72.3581 \pm 6.3152$ nm. The lattice strain (ε) was calculated using the S–W, W–H's UDM, SSP, and H–W methods to be $\simeq -0.1558 \times 10^{-3} \pm 25.3500 \times 10^{-6}$. In $CdIn_2Se_4$, it was found that the root mean square strain (ε_{rms}) varies linearly with lattice strain (ε), indicating a consistent crystallographic orientation of the lattice planes. Dislocation density (δ) was calculated using the W–S method ($\simeq 0.2163 \times 10^{-3}$ lines nm^{-2}). The lattice stress (σ) was calculated using W–H's USDM approach to be $\simeq -2.8496 \times 10^6$ Pa. W–H's UDEDM-derived energy density (u) is $\simeq 0.1860 \times 10^3$ J m^{-3}. Bulk modulus (B_H) ($\simeq$40.7787 GPa), shear modulus (G_H) ($\simeq$15.5735 GPa), Young's modulus (y) ($\simeq$41.4445 GPa), Poisson's ratio (ν) ($\simeq$0.3306), elastic anisotropy, melting temperature (T_m) ($\simeq 598.4678 \pm 300$ K), transverse sound velocity (ν_t) ($\simeq$1.6749 km s^{-1}), longitudinal sound velocity (ν_l) ($\simeq$3.3296 km s^{-1}), average wave velocity (ν_m) ($\simeq$1.8783 km s^{-1}), and Debye temperature (θ_D) ($\simeq$183.9084 K) were also determined for $CdIn_2Se_4$. The stoichiometry and elemental distribution of the synthesized $CdIn_2Se_4$ compound were confirmed by EDAX, whereas the density (ρ) (5551.2204 kg m^{-3}) was confirmed using a pycnometer. Through the use of room-temperature (RT) ($\simeq$300 K) FTIR spectroscopy in the wavenumber ($\bar{\nu}$) range of 4000–400 cm^{-1}, the lack of functional groups in the FTIR spectra verified the purity of the synthesized $CdIn_2Se_4$ compound.

Data availability

The authors declare that the data supporting the findings of this study are available in the main text of the paper.

Author contributions

All authors contributed to the study's conception and design. Material preparation, data collection, and analysis were carried out by S. D. Dhruv, Sergei A. Sharko, Aleksandra I. Serokurova, Nikolai N. Novitskii, D. L. Goroshko, Parth Rayani, Jagruti Jangale, Naveen Agrawal, Vanaraj Solanki, J. H. Markna, Bharat Kataria, and D. K. Dhruv. D. K. Dhruv wrote the first draft of the manuscript, and all authors reviewed and commented on previous versions. All authors read and approved the final manuscript. S. D. Dhruv: data curation, Sergei A. Sharko: conceptualization, Aleksandra I. Serokurova: investigation, Nikolai N. Novitskii: formal analysis, D. L. Goroshko: visualization, Parth Rayani: writing-review & editing, Jagruti Jangale: resources, Naveen Agrawal: validation, Vanaraj Solanki: methodology, J. H. Markna: software, Bharat Kataria: project administration, D. K. Dhruv: writing-original draft, supervision.

Conflicts of interest

The submitted work is the authors' original research and has not been submitted elsewhere for publication. On behalf of all co-authors, I declare that there are no conflicts of interest.

Acknowledgements

The work was supported by the Department of Science & Technology (DST), Government of India, New Delhi (File number: DST/INT/BLR/P-36/2023), and the Belarusian Republican Foundation for Fundamental Research (File number:

F23IND-005) under the India–Belarus Programme of Co-operation in Science & Technology (Joint Research Project). The authors thank the Science and Technology Facilities Council (STFC) for providing access to the CASTEP code for computational work. The authors also express their gratitude to the Sophisticated Instrumentation Centre for Applied Research and Testing (SICART), Vallabh Vidyanagar-388120, Anand, Gujarat, India, for providing access to discounted X-ray diffraction (XRD), energy-dispersive X-ray analysis (EDAX), and Fourier transform infrared (FTIR) spectroscopy facilities.

References

1 S. I. Radautsan, A. N. Georgobiani and I. M. Tiginyanu, *Prog. Cryst. Growth Charact.*, 1984, **10**, 403–412.
2 E. F. M. El-Zaidia, E. A. El-Shazly and H. A. M. Ali, *J. Inorg. Organomet. Polym.*, 2020, **30**, 2979–2986.
3 D. Santamaría-Pérez, O. Gomis, A. L. J. Pereira, R. Vilaplana, C. Popescu, J. A. Sans, F. J. Manjón, P. Rodríguez-Hernández, A. Muñoz, V. V. Ursaki and I. M. Tiginyanu, *J. Phys. Chem. C*, 2014, **118**, 26987–26999.
4 D. K. Dhruv, B. H. Patel, S. D. Dhruv, P. B. Patel, U. B. Trivedi and N. Agrawal, *Mater. Today: Proc.*, 2023, S2214785323002638.
5 S. D. Dhruv, J. Kolte, P. Solanki, V. Solanki, J. H. Markna, B. Kataria, B. A. Amin, N. Agrawal and D. K. Dhruv, *Interactions*, 2024, **245**, 99.
6 A. N. Georgobiani, B. G. Tagiev, O. B. Tagiev, R. B. Djabbarov, N. N. Musaeva and U. F. Kasumov, *Jpn. J. Appl. Phys.*, 2000, **39**, 434.
7 D. K. Dhruv, B. H. Patel and D. Lakshminarayana, *Mater. Res. Innovations*, 2016, **20**, 285–292.
8 D. K. Dhruv, B. H. Patel, N. Agrawal, R. Banerjee, S. D. Dhruv, P. B. Patel and V. Patel, *J. Mater. Sci.: Mater. Electron.*, 2022, **33**, 24003–24015.
9 D. K. Dhruv, A. Nowicki, B. H. Patel and V. D. Dhamecha, *Surf. Eng.*, 2015, **31**, 556–562.
10 V. Dhamecha, B. Patel, D. Dhruv and A. Nowicki, *Surf. Eng.*, 2020, **36**, 100–105.
11 M. Tomkiewicz, W. Siripala and R. Tenne, *J. Electrochem. Soc.*, 1984, **131**, 736–740.
12 M. M. El-Nahass, *Appl. Phys. A*, 1991, **52**, 353–357.
13 H. Neumann, W. Kissinger, F. Lévy, H. Sobotta and V. Riede, *Cryst. Res. Technol.*, 1990, **25**, 1455–1459.
14 H. Neumann, W. Kissinger and F. Lévy, *Cryst. Res. Technol.*, 1990, **25**, 1189–1193.
15 C. Razzetti, T. Besagni, S. Bini and P. P. Lottici, *Phys. Status Solidi A*, 1989, **111**, 411–416.
16 L. Fornarini, F. Stirpe, E. Cardarelli and B. Scrosati, *Solar Cells*, 1984, **11**, 389–400.
17 R. Trykozko and D. R. Huffman, *J. Appl. Phys.*, 1981, **52**, 5283–5285.
18 G. Margaritondo, A. D. Katnani and F. Lévy, *Phys. Status Solidi B*, 1981, **103**, 725–731.
19 J. Przedmojski and B. Pałøz, *Phys. Status Solidi A*, 1979, **51**, K1–K3.
20 K. Adpakpang, T. Sarakonsri, S. Isoda, Y. Shinoda and C. Thanachayanont, *J. Alloys Compd.*, 2010, **500**, 259–263.
21 A.-A. Ruanthon, T. Sarakonsri and C. Thanachayanont, *Funct. Mater. Lett.*, 2009, **02**, 199–203.
22 S.-H. Choe, B.-N. Park, K.-S. Yu, S.-J. Oh, H.-L. Park and W.-T. Kim, *J. Phys. Chem. Solids*, 1995, **56**, 89–92.
23 T. G. Kerimova, F. R. Adzalova, R. Kh. Nani and V. Ya. Shteinshreiber, *Phys. Status Solidi A*, 1981, **67**, K143–K146.
24 E. Guerrero, M. Quintero and J. C. Woolley, *J. Phys.: Condens. Matter*, 1990, **2**, 6119–6126.
25 E. Fortin and F. Raga, *Solid State Commun.*, 1974, **14**, 847–850.
26 R. Nitsche, *J. Phys. Chem. Solids*, 1960, **17**, 163–165.
27 I. A. Mamedova, Z. A. Jahangirli, T. G. Kerimova and N. A. Abdullayev, *Phys. Status Solidi B*, 2023, **260**, 2200441.
28 S. Chandra, A. Sinha and V. Kumar, *Int. J. Mod. Phys. B*, 2019, **33**, 1950340.
29 A. Priyambada, A. Mohanty and P. Parida, *Mater. Today Commun.*, 2023, **37**, 107338.
30 D. M. Hoat, M. Naseri, R. Ponce-Pérez, J. F. Rivas-Silva and G. H. Cocoletzi, *J. Solid State Chem.*, 2020, **282**, 121078.
31 V. M. Nikale, S. S. Shinde, A. R. Babar, C. H. Bhosale and K. Y. Rajpure, *Sol. Energy*, 2011, **85**, 1336–1342.
32 V. M. Nikale, S. S. Shinde, A. R. Babar, C. H. Bhosale and K. Y. Rajpure, *Sol. Energy*, 2011, **85**, 325–333.
33 V. M. Nikale, S. S. Shinde, A. R. Babar, C. H. Bhosale and K. Y. Rajpure, *Appl. Sol. Energy*, 2010, **46**, 194–201.
34 R. Tenne, Y. Mirovsky, G. Sawatzky and W. Giriat, *J. Electrochem. Soc.*, 1985, **132**, 1829–1835.
35 R. Tenne, Y. Mirovsky, Y. Greenstein and D. Cahen, *J. Electrochem. Soc.*, 1982, **129**, 1506–1512.
36 V. Nikale, *Sol. Energy Mater. Sol. Cells*, 2004, **82**, 3–10.
37 S. J. Clark, M. D. Segall, C. J. Pickard, P. J. Hasnip, M. I. J. Probert, K. Refson and M. C. Payne, *Z. Kristallogr. Cryst. Mater.*, 2005, **220**, 567–570.
38 W. Bao, D. Liu, P. Li and Y. Duan, *Ceram. Int.*, 2019, **45**, 1857–1867.
39 K. Wark, *Thermodynamics*, McGraw-Hill, New York, 5th edn, 1988.
40 T. Takizawa, C. Komatsu-Hidaka, K. Asaka, T. Isomoto and H. Matsushita, *Jpn. J. Appl. Phys.*, 2000, **39**, 35.
41 B. D. Cullity and S. R. Stock, *Elements of X-ray Diffraction*, Prentice Hall, Upper Saddle River, NJ, 3rd edn, 2001.
42 H. Hahn, G. Frank, W. Klingler, A. D. Störger and G. Störger, *Z. Anorg. Allgem. Chem.*, 1955, **279**, 241–270.
43 R. Suresh, V. Ponnuswamy and R. Mariappan, *Appl. Surf. Sci.*, 2013, **273**, 457–464.
44 S. D. Dhruv, J. Kolte, P. Solanki, M. P. Deshpande, V. Solanki, J. Tailor, N. Agrawal, V. A. Patel, J. H. Markna, B. Kataria and D. K. Dhruv, *RSC Adv.*, 2024, **14**, 15455–15467.
45 V. M. Nikale, S. S. Shinde, C. H. Bhosale and K. Y. Rajpure, *J. Alloys Compd.*, 2011, **509**, 3116–3121.
46 S. D. Dhruv, J. Kolte, P. Solanki, S. A. Sharko, V. Solanki, J. Tailor, K. Chaudhari, N. Agrawal, V. A. Patel, J. H. Markna, B. Kataria and D. K. Dhruv, *J. Mater. Sci.: Mater. Electron.*, 2024, **35**, 1202.

47 M. Zhang, Y. Chen, C. Qiu, X. Fan, C. Chen and Z. Wang, *Phys. E*, 2014, **64**, 218–223.
48 B. G. Wagh, A. B. Bhalerao, R. N. Bulakhe and C. D. Lokhande, *Mod. Phys. Lett. B*, 2015, **29**, 1540024.
49 M. A. M. Seyam, G. F. Salem and S. N. A. Aziz, *J. Sol.*, 2011, **34**, 88–98.
50 O. Madelung, *Semiconductors: Data Handbook*, Springer Berlin Heidelberg, Berlin, Heidelberg, 2004.
51 J.-H. Ahn, G. Cai, R. S. Mane, V. V. Todkar, A. V. Shaikh, H. Chung, M.-Y. Yoon and S.-H. Han, *Appl. Surf. Sci.*, 2007, **253**, 8588–8591.
52 A. B. Bhalerao, B. G. Wagh, R. N. Bulakhe, P. R. Deshmukh, J.-J. Shim and C. D. Lokhande, *J. Photochem. Photobiol. A Chem.*, 2017, **336**, 69–76.
53 V. M. Nikale, U. B. Suryavanshi and C. H. Bhosale, *Mater. Sci. Eng., B*, 2006, **134**, 94–98.
54 K. Momma and F. Izumi, *J. Appl. Crystallogr.*, 2011, **44**, 1272–1276.
55 O. Singh, A. Agarwal, S. Sanghi and J. Singh, *Int. J. Appl. Ceram. Technol.*, 2019, **16**, 119–129.
56 A. El-Habib, M. Addou, A. Aouni, M. Diani, J. Zimou and H. Bakkali, *Materialia*, 2021, **18**, 101143.
57 Y. Canchanya-Huaman, A. F. Mayta-Armas, J. Pomalaya-Velasco, Y. Bendezú-Roca, J. A. Guerra and J. A. Ramos-Guivar, *Nanomaterials*, 2021, **11**, 2311.
58 C. M. Magdalane, K. Kaviyarasu, J. J. Vijaya, B. Siddhardha and B. Jeyaraj, *J. Photochem. Photobiol. B*, 2016, **163**, 77–86.
59 B. Parveen, M. Hassan, Z. Khalid, S. Riaz and S. Naseem, *J. Appl. Res. Eng. Technol.*, 2017, **15**, 132–139.
60 P. Shunmuga Sundaram, T. Sangeetha, S. Rajakarthihan, R. Vijayalaksmi, A. Elangovan and G. Arivazhagan, *Phys. B*, 2020, **595**, 412342.
61 M. Rabiei, A. Palevicius, A. Monshi, S. Nasiri, A. Vilkauskas and G. Janusas, *Nanomaterials*, 2020, **10**, 1627.
62 A. Monshi, M. R. Foroughi and M. R. Monshi, *World J. Nano Sci. Eng.*, 2012, **02**, 154–160.
63 D. Nath, F. Singh and R. Das, *Mater. Chem. Phys.*, 2020, **239**, 122021.
64 B. Himabindu, N. S. M. P. Latha Devi and B. Rajini Kanth, *Mater. Today: Proc.*, 2021, **47**, 4891–4896.
65 K. B. Vinjamuri, S. Viswanadha, H. Basireddy and R. K. Borra, *Appl. Mech. Mater.*, 2021, **903**, 27–32.
66 M. Basak, Md. L. Rahman, Md. F. Ahmed, B. Biswas and N. Sharmin, *J. Alloys Compd.*, 2022, **895**, 162694.
67 M. P. Deshpande, N. Garg, S. V. Bhatt, B. Soni and S. H. Chaki, *Adv. Mater. Res.*, 2013, **665**, 267–282.
68 S. Singh, M. C. Rath, A. K. Singh, T. Mukherjee, O. D. Jayakumar, A. K. Tyagi and S. K. Sarkar, *Radiat. Phys. Chem.*, 2011, **80**, 736–741.
69 Y. Wen, X. Zeng, Z. Hu, R. Peng, J. Sun and L. Song, *Intermetallics*, 2018, **101**, 72–80.
70 J. W. Yang and H. J. Hou, *High Pressure Res.*, 2012, **32**, 376–384.
71 P. Govindaraj, M. Sivasamy, K. Murugan, K. Venugopal and P. Veluswamy, *RSC Adv.*, 2022, **12**, 12573–12582.
72 K. B. Panda and K. S. Ravi Chandran, *Comput. Mater. Sci.*, 2006, **35**, 134–150.
73 Z. H. Mahmoud, Y. Ajaj, A. M. Hussein, H. N. K. Al-Salman, M. A. Mustafa, E. H. Kadhum, S. Abdullaev, S. A. Khuder, G. K. Ghadir, S. M. Hameed, K. Muzammil, S. Islam and E. Kianfar, *Int. J. Biol. Macromol.*, 2024, **267**, 131465.